Atmos. Chem. Phys., 25, 15487–15506, 2025 https://doi.org/10.5194/acp-25-15487-2025 © Author(s) 2025. This work is distributed under the Creative Commons Attribution 4.0 License.





Urban-rural patterns and driving factors of particulate matter pollution decrease in eastern China

Zhihao Song^{1,2} and Bin Chen^{1,2}

¹College of Atmospheric Sciences, Lanzhou University, Lanzhou 730000, China ²Institute of Meteorological Artificial Intelligence Research, Lanzhou University, Lanzhou 730000, China

Correspondence: Bin Chen (chenbin@lzu.edu.cn)

Received: 10 May 2025 – Discussion started: 6 June 2025 Revised: 23 September 2025 – Accepted: 24 September 2025 – Published: 13 November 2025

Abstract. Understanding the urban-rural patterns and driving drivers behind the recent decrease in particulate matter (PM) pollution across eastern China is essential for assessing the efficacy of environmental policies and ensuring equitable health co-benefits. By employing an interpretable, end-to-end machine learning framework integrating satellite observations, meteorological factors, and auxiliary datasets, this study reveals changes in urban and rural PM pollution and the underlying drivers. During the period 2015–2023, the average decrease rates of PM_{10} and $PM_{2.5}$ in eastern China were -4.02 ± 1.29 and $-2.41\pm0.91\,\mu\text{g m}^{-3}\,\text{yr}^{-1}$, respectively. The rate of decrease in urban areas was higher than that in rural areas, which played a dominant role in PM reduction. Significant reductions in PM concentrations were observed in urban core areas, suburbs, towns and regions with high agricultural pressure. The interpretability analysis showed that temperature and interannual variability were the main drivers of PM pollution reduction. However, only interannual variability showed a significant decreasing trend in its effect on PM pollution, while other driving factors showed periodic variations. Furthermore, there were differences in the drivers of PM reduction between urban and rural areas, particularly with interannual variability in particular contributing to PM pollution reduction in urban areas, but having a lesser impact in most rural areas. This study reveals the urban-rural patterns of PM pollution reduction in eastern China, and highlights the need for differentiated air pollution control strategies in urban and rural areas.

1 Introduction

Air pollution caused by $PM_{2.5}$ and PM_{10} (airborne particulate matter with diameters less than 2.5 µm and 10 µm, respectively) has adversely affected China's atmospheric environment (Huang et al., 2014a; Zhang et al., 2012). PM pollution is now considered the greatest environmental risk factor for global human health (Apte et al., 2015), as exposure to PM can trigger various respiratory and cardiovascular diseases (Burnett Richard et al., 2014; West et al., 2016; Cohen et al., 2017). The indirect health risks associated with PM exposure (Yin et al., 2020) contribute to millions of premature deaths annually in China (Burnett et al., 2018). To mitigate the escalating risks of particulate matter exposure and reduce the public health burden, the Chinese government introduced the "Air Pollution Prevention and Control Action Plan" in 2013 (State Council of the People's Repub-

lic of China, 2013). This initiative aims to implement policies to improve energy efficiency, reduce energy-related pollution, and curb anthropogenic emissions to control particulate matter pollution in the atmosphere (State Council of the People's Republic of China, 2014). As a result of this initiative, China's atmospheric particulate matter pollution has improved significantly (Cheng et al., 2021). Between 2013 and 2017, the annual average concentration of PM_{2.5} decreased by 28 %-40 % (Zheng et al., 2018; Ministry of Ecology and Environment of the People's Republic of China, 2017), and the population-weighted national annual average concentration of PM_{2.5} decreased by 32 % (Xue et al., 2019). Data from the National Air Quality Monitoring Network show that between 2013 and 2020, the annual average PM_{2.5} concentration in urban areas of China decreased from 72 to $33 \,\mu\mathrm{g}\,\mathrm{m}^{-3}$ (Song et al., 2023). As a result, the Clean Air Action has achieved remarkable results in reducing PM pollution (Zhang et al., 2019b).

It is widely accepted that improvements in air quality can be attributed to both reductions in anthropogenic emissions (Geng et al., 2019; Zheng et al., 2023; Zhao et al., 2018) and changes in meteorological conditions (An et al., 2019; Cao and Yin, 2020; Chen et al., 2020a). To assess the driving factors behind changes in PM concentration trends, it is essential to distinguish between anthropogenic emissions and meteorological factors (Zhong et al., 2018). Zhong et al. (2021) found that PM_{2.5} concentrations decreased by 44 % from 2013 to 2019, and by 34 % when the influence of meteorological conditions was excluded, thus demonstrating the effectiveness of emission reduction measures. Qiu et al. (2022) used the GEOS-Chem chemical transport model to simulate the impact of anthropogenic emissions on PM pollution trends and provided recommendations for attributing PM pollution trends to emission changes. Vu et al. (2019) used machine learning to assess the impact of air quality trends in Beijing and found that PM_{2.5} and PM₁₀ concentrations decreased by 34 % and 24 %, respectively, after excluding meteorological influences, attributing the decrease to reduced coal burning. Zhai et al. (2019) used a stepwise multiple linear regression (MLR) model to quantify PM_{2.5} trends in China between 2013 and 2018, and found that meteorological conditions contributed about 12 %. However, Xiao et al. (2021) used statistical methods to separate the contributions of emissions and meteorology to long-term PM_{2.5} trends in East China, and found that meteorological contributions were even higher in certain years. Overall, distinguishing the contributions of anthropogenic emissions and meteorological changes to PM pollution is crucial to improve understanding of pollution processes and to inform pollution control policies and future air quality predictions.

However, the urban-rural patterns of PM pollution improvement remain poorly understood in existing research (Chen et al., 2020b). Many studies on PM pollution either focus on highly polluted regions (such as the Beijing-Tianjin-Hebei region) (Chen et al., 2019b, c), or on developed regions with a high concentration of large cities (such as the Yangtze River Delta and the Pearl River Delta) (Gui et al., 2019; He et al., 2017). This focus is mainly due to the high concentrations of air pollutants in developed cities (Sicard et al., 2023), where PM pollution poses a significant public health threat to densely populated urban areas (Brauer et al., 2016; Southerland et al., 2022). Although PM pollution in urban areas highlights the importance of environmental governance, rural areas, with different consumption habits and living conditions (e.g., solid fuel burning in households) (Li et al., 2014), may experience air pollution that differs from urban areas (Wang et al., 2024a). In certain seasons and regions, PM exposure factors in rural areas are generally higher than those in urban areas, with exposure levels reaching up to 70 % (Wang et al., 2024b). Therefore, the contribution of these regions to PM pollution improvement may differ (Li et al., 2024b). Without targeted assessments, perceptions of the relative importance of urban and rural areas in China's air pollution control efforts may be distorted, hindering the development of appropriate environmental policies and the promotion of green development in urban and rural construction (Yang et al., 2024).

Currently, many studies have used machine learning models to obtain particulate matter concentration products and apply them to pollution assessment (Chen et al., 2019a; Huang et al., 2021). Among these, extreme tree models and data from the Himawari-8 satellite have demonstrated outstanding performance (Wei et al., 2021b, a, c). In particular, the extreme tree model demonstrates its unique advantages, including greater randomness and interference resistance, and outperforms other similar models in terms of performance (Wei et al., 2023). This study advances the understanding of the current status and driving factors of urbanrural PM pollution improvement using interpretable machine learning methods. First, by integrating Himawari-8/9 satellite top-of-atmosphere reflectance (TOAR) data, meteorological data, and geographic information, we use a multiple-output extreme trees (MOET) model to capture the spatiotemporal distribution of PM (including PM₁₀ and PM_{2.5}) across China and assess the patterns of PM pollution improvement. We then use various machine learning interpretability techniques, such as relative importance, tree interpreters, and SHAP values, to quantify the contributions of anthropogenic emissions and meteorological changes to PM pollution improvement. To investigate potential differences in the results between urban and rural areas, we use land use data to distinguish urban from rural regions in eastern China. This study aims to address the following three questions: (1) What are the spatio-temporal patterns of PM pollution improvement in urban and rural areas of China? (2) What are the main driving factors behind the differences in PM pollution improvement between urban and rural areas? (3) What are the specific contributions of each driving factor to PM pollution improvement? Answering these questions is crucial for a comprehensive understanding of the dynamics of urban and rural atmospheric particulate pollution control in China.

2 Data and Methods

2.1 Satellite TOAR data and ground-based PM observations

Previous studies have shown that satellite-observed top-of-atmosphere reflectance (TOAR) data can be used to estimate near-surface air pollutants (Chen et al., 2024a; Yang et al., 2023; Song et al., 2024). In particular, the TOAR data from the Himawari-8 satellite have demonstrated excellent performance in pollutant estimation (Hu et al., 2022; Liu et al., 2019). The Advanced Himawari Imager (AHI) on board the Himawari-8/9 satellite is an advanced passive observation instrument with 16 observation channels, provid-

ing a spatiotemporal resolution of up to 10 min and 0.5 km (Bessho et al., 2016). Based on the sensitivity of the AHI sensor (Yoshida et al., 2018), three visible channels (0.46, 0.51, and 0.64 µm) and two near-infrared channels (0.86 and 2.3 µm) were used in this study. In addition, four angles related to aerosol inversion results: SAA (satellite azimuth angle), SAZ (satellite zenith angle), SOA (solar azimuth angle), and SOZ (solar zenith angle) were also included in the study. TOAR data from the AHI imager were obtained from the Himawari Monitor P-Tree System data download website of the Japan Meteorological Agency (https://www.eorc.jaxa.jp/ptree/index.html, last access: 20 September 2025, JMA, 2025). The time range for Himawari-8 data is from 1 September 2015, to 30 September 2022, while the time range for Himawari-9 data is from 1 October 2022, to 31 August 2023.

The ground-based PM data were provided by the China National Environmental Monitoring Center (CNEMC) (http://www.cnemc.cn, last access: 20 September 2025) and were calibrated and quality controlled according to the Chinese National Standard GB 3095-2012 (Ministry of Ecology and Environment of the People's Republic of China, 2012). In this study, hourly mean PM₁₀ and PM_{2.5} data were collected from approximately 1400 stations in eastern China (102–136° E, 16–56° N) for the period from 1 September 2015 to 31 August 2023. Observations with PM_{2.5} concentrations above 600 μg m⁻³ or PM₁₀ concentrations above 1000 μg m⁻³, as well as those with concentrations below 1 μg m⁻³, were excluded (Shi et al., 2024).

2.2 Meteorological data and geographic information data

Studies assessing the impact of meteorological factors on PM pollution have identified temperature, humidity, and wind as the main variables influencing PM2.5 concentrations, with their effects significantly outweighing those of other factors. Among these, temperature has the most significant and stable influence (Chen et al., 2018b). In this study, meteorological data were obtained from the ERA-5 reanalysis dataset provided by the European Centre for Medium-Range Weather Forecasts (https://cds.climate.copernicus.eu/cdsapp#!/dataset/, access: 20 September 2025). The dataset includes boundary layer height (BLH), relative humidity (RH), surface pressure (SP), 2 m air temperature (T2M), wind direction (WD), wind speed (WS), and net solar radiation at the surface (NSR), with spatial resolutions of $0.1^{\circ} \times 0.1^{\circ}$ or $0.25^{\circ} \times 0.25^{\circ}$ (Hersbach et al., 2020). Geographic information can also influence pollutant concentrations to some extent due to variations in meteorological conditions (Chen et al., 2018a; Chen et al., 2021). The geographic information data used in this study include elevation (HEIGHT), land cover type (LUCC), and population density (RK). HEIGHT is derived from SRTM-3 elevation data, with a spatial resolution of 90 m and a temporal resolution of 1 year. The download URL is https://doi.org/10.5067/MEaSUREs/SRTM/SRTMGL3.003 (NASA JPL, 2013). LUCC is sourced from the dataset (MCD12Q1), with a spatial resolution of 500 m and a temporal resolution of 1 year. The download URL is https://doi.org/10.5067/MODIS/MCD12Q1.006 (NASA Land Processes Distributed Active Archive Center, 2019), used to describe land surface types and land use conditions. RK is derived from the 2015 United Nations adjusted population density data, with a spatial resolution of 0.1° × 0.1° and a temporal resolution of 1 year, available at https://doi.org/10.7927/H4PN93PB (Center For International Earth Science Information Network-CIESIN-Columbia University, 2018). It is provided by the Social and Economic Data and Applications Center (SEDAC) of the National Aeronautics and Space Administration (NASA).

2.3 Data integration and development of the Multiple-Output Extreme Trees Model

The resolution of the meteorological and geographic information data was adjusted to $0.05^{\circ} \times 0.05^{\circ}$ using bilinear interpolation. All data were then matched with station data according to the $0.05^{\circ} \times 0.05^{\circ}$ grid of the Himawari-8 satellite. The specific matching method is described in detail in Chen et al. (2022c) and Song et al. (2022b).

The DOET model is developed on the basis of the Extreme Trees (ET) model (Geurts et al., 2006), which is capable of simultaneously handle multi-target variable output tasks. The ET model is similar to the Random Forest (RF) model, both of which consist of multiple decision trees. However, whereas the RF model randomly samples data with replacement, the ET model uses all available samples. After determining the samples and features, the ET model constructs decision trees based on optimal partition attributes. This process is repeated until a sufficient number of decision trees have been constructed to form the ET model. Finally, the average regression results of all decision trees in the ET are used as the final output. Several studies have confirmed that the ET model has excellent fitting performance (Qin et al., 2020; Zhang et al., 2022a; Chen et al., 2022a).

In this study, three model parameters were optimized: the number of trees (n_estimators), the maximum depth of the model (max_depth), and the minimum number of samples required to split a node (min_samples_split). After balancing the accuracy and efficiency of the model, these parameters were set to 70, 100, and 5, respectively. The model, which uses satellite observations, meteorological data, and geographical information to estimate near-surface PM concentrations, can be expressed as:

$$(PM_{10}, PM_{2.5}) =$$

$$f \begin{pmatrix} TOAR_{1,2,3,4,6}, BLH, RH, SP, T2M, WD, WS, NSR, \\ Height, LUCC, RK, \\ year, mon, doy, hour, lon, lat, SAA, SAZ, SOA, SOZ \end{pmatrix}$$
 (1)

Here, f represents the DOET model, and TOAR_{1,2,3,4,6} denotes the radiance values of the three visible channels (0.46,

0.51, and 0.64 µm) and the two near-infrared channels (0.86 and 2.3 µm). BLH, RH, SP, T2M, WD, WS and NSR are meteorological variables, while Height, LUCC and RK represent geographical information. The variables lon (Longitude), lat (Latitude), SAA, SAZ, SOA and SOZ representing spatial information. The variables year, mon (month), doy (day of the year), and hour are temporal information reflecting the influence of anthropogenic emissions on PM pollution (Wei et al., 2020). Time variables (year, month) effectively characterize cyclical patterns and long-term trends in human activity, serving as reliable proxy indicators in pollution analysis (Song et al., 2023). Monthly cycles directly reflect seasonal rhythms: winter heating spikes PM_{2.5} and SO2 levels (Liu et al., 2017), agricultural phases amplify ammonia emissions (Ma et al., 2025), and transportation peaks during holidays elevate NO2 concentrations (Hua et al., 2021). Annual trends capture industrial evolution and policy impacts, such as the PM_{2.5} reduction after implementing the "Air Pollution Prevention Action Plan" (Geng et al., 2024; Geng et al., 2021). As standardized, quantifiable metrics, time variables circumvent data limitations for complex activities (e.g., energy consumption, economic behaviors, urban sprawl), enable cross-regional comparisons without normalization, and reveal pollution responses to socioeconomic rhythms and policy efficacy (Dai et al., 2021; Shi et al., 2021). Specifically, year and month (mon) are used to represent the interannual and intra-annual variations in anthropogenic emissions, respectively (Zhang et al., 2019a; Park et al., 2019). The estimation workflow is illustrated in Fig. 1. The specific estimation process of the DOET model is as follows: firstly, meteorological factors, geographic information, and satellite TOAR data are input into the DOET model and matched with PM observation data. Then, the DOET model fits the PM observation data with the input variables to obtain two ET estimation models (PM₁₀ and PM_{2.5}). Finally, the two ET models are integrated to obtain the DOET model, and the estimation results of PM₁₀ and PM_{2.5} are output simultaneously to save computation time. Finally, the obtained PM₁₀ and PM_{2.5} data are subjected to further analysis. Additionally, we performed weather normalization on the PM data to mitigate the impact of meteorological events (Grange and Carslaw, 2019).

Model performance was evaluated using 10-fold cross-validation (Rodriguez et al., 2010), incorporating sample-based, space-based, and time-based validation methods (Wei et al., 2019). Evaluation metrics used included the coefficient of determination (R^2), root mean square error (RMSE), and mean absolute error (MAE) for both PM₁₀ and PM_{2.5} (Chen et al., 2023).

$$R^2 = 1 - \frac{\text{ss}_{\text{res}}}{\text{SS}_{\text{tot}}} \tag{2}$$

$$MAE = \frac{1}{n} \sum_{i=1}^{n} |\hat{y}_i - y_i|$$
 (3)

RMSE =
$$\sqrt{\frac{1}{n} \sum_{i=1}^{n} (\hat{y}_i - y_i)^2}$$
 (4)

In Eq. (2), ss_{res} represents the error between the estimated value of the model and the average value of the observed values of PM_{10} and $PM_{2.5}$, SS_{tot} represents the error between the observed values of PM_{10} and $PM_{2.5}$ and the average value of the observed values of PM_{10} and $PM_{2.5}$ from CNEMC. In Eqs. (3)–(5), $\hat{y_i}$ represents the PM_{10} and $PM_{2.5}$ estimated value of the DOET model, y_i represents the observed value of PM_{10} and $PM_{2.5}$ from CNEMC.

2.4 Machine learning interpretability variables

To investigate the influence of potential driving factors on PM pollution improvement in eastern China, we employed relative importance (Berner et al., 2020), tree interpreter (Wang et al., 2022b), and SHapley Additive exPlanations (SHAP) (Lundberg and Lee, 2017) to distinguish the contributions of meteorological changes and anthropogenic emissions to PM pollution improvement. Relative importance was assessed using the permutation importance value of the DOET model, defined as the average reduction in model accuracy when a single feature value is randomly shuffled (Yang et al., 2022).

The permutation importance of each variable was calculated using the "permutation_importance" library in Python. To reduce uncertainty, the training process was repeated 20 times for each grid point to obtain robust estimates of relative importance (Qu et al., 2023). The tree interpreter was applied using the "tree_interp_functions" library in Python, which is designed for predictions based on decision tree ensemble models and facilitates the decomposition of each prediction into bias and feature contribution components. The detailed calculation method and code for the tree interpreter can be obtained from the following URL: https://github.com/andosa/treeinterpreter/tree/master (last access: 20 September 2025).

SHAP values are based on Shapley value theory, which explains model predictions by calculating the relative contribution of each feature to the output (He et al., 2024). These values reflect not only the influence of features on individual samples but also indicate the positive and negative contributions of these influences. SHAP explanations can be applied to any machine learning model, including neural networks and ensemble models, and provide comprehensive and accurate interpretability results. Thus, the SHAP method provides superior explanations for both local and global model effects

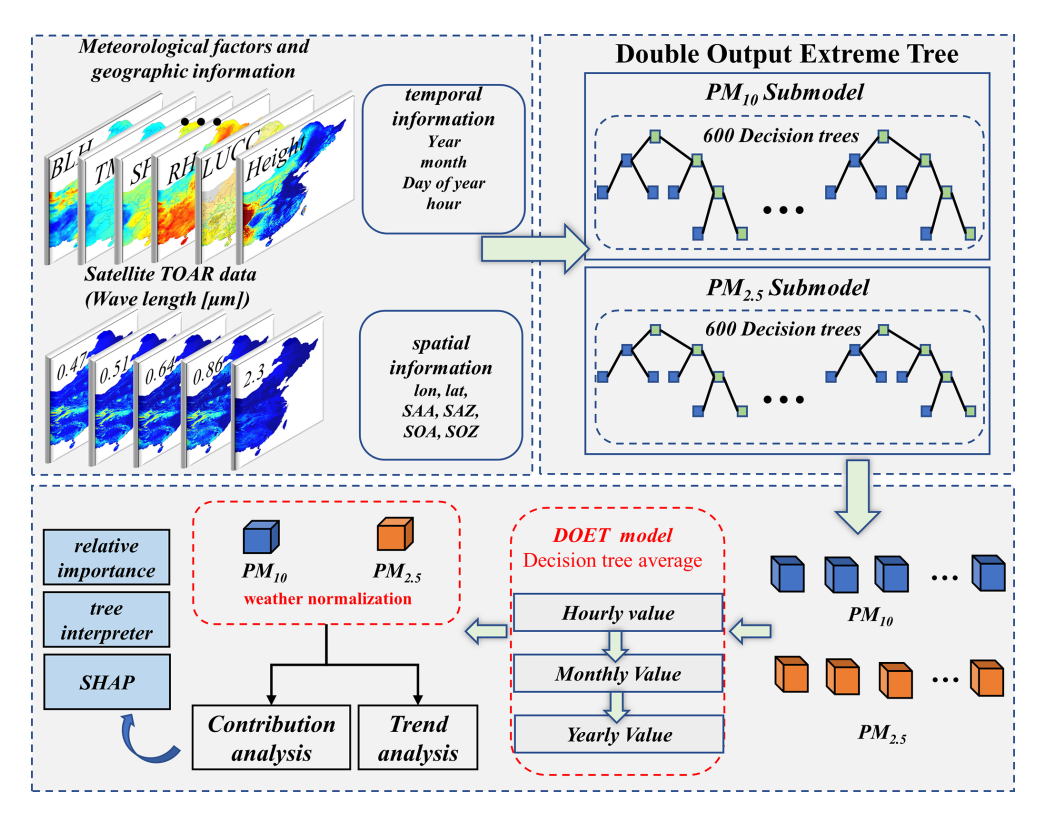


Figure 1. Workflow of PM data estimation and pollution driving factors assessment.

(Liu et al., 2023; Hou et al., 2022). In Python, "tree_SHAP" is specifically tailored for decision tree-based machine learning models, such as the Extreme Tree model, to provide greater accuracy and faster computation.

The interpretability variables described above were applied to the monthly averaged PM₁₀ and PM_{2.5} datasets generated by the DOET model.

2.5 Land cover type classification

Zhang et al. (2022b) proposed a method to differentiate urban and rural areas based on the gradient of human land use pressure. In this study, the MCD12Q1 land cover map, with a spatial resolution of $500\,\mathrm{m}$ was used. For grids measuring $5\times 5\,\mathrm{km}$, urban and rural classifications were determined by the coverage of specific land cover categories (e.g., urban land and cropland), which reflect the transition from urban to rural areas and correspond to different levels of human activity. As shown in Table 1 and Fig. S1 in the Supplement, urban areas in this study include both urban core areas and suburban regions, while rural areas are categorized into six types: towns, high agricultural pressure areas, low agricultural pressure areas, forests and grasslands.

3 Results

3.1 PM estimation model performance and PM distribution characteristics

For the period from September 2015 to August 2023 in eastern China, a total of 6772429 samples were matched. After parameter optimization and feature training, the optimal DOET model was derived, and long-term time-series spatial distribution products for PM₁₀ and PM_{2.5} in eastern China were generated. Figure 2 shows the results of 10-fold crossvalidation based on sample, spatial and temporal validations. Overall, the DOET model showed a high level of accuracy in the estimation of PM data. The sample-based 10-fold crossvalidation results (Fig. 2c and f) yielded an R^2 of 0.87, with RMSE (MAE) values of 25.82 (14.87) μ g m⁻³ for PM₁₀ and $14.36 (8.44) \, \mu g \, m^{-3}$ for $PM_{2.5}$. The slope of the fitting line between observed and estimated values was 0.84. The performance of the DOET model in this study is comparable to that reported in other studies that estimated PM using Himawari-8 TOAR data (Wang et al., 2021; Chen et al., 2024b; Yin et al., 2021).

The 10-fold cross-validation results based on spatial and temporal validation were slightly lower than those based on samples (Fig. 2d–e and g–h). Spatial validation assessed the performance of the model in estimating PM concentrations in areas without monitoring stations, after training the model with samples from areas with stations. Temporal validation

Table 1. Definitions of urban and rural land cover classes.

Urban-Rural Land Cover Class	Definition
Urban	50 % < Urban grid
Suburban	25 % < Urban grid < 50 %
Towns	12.5 % < Urban grid < 25 %
High Agricultural Pressure Areas	50 % < Cropland grid
Low Agricultural Pressure Areas	12.5 % < Cropland grid grid < 50 %
Forests	50 % < Forest grid
Grasslands	50 % < Grassland grid
Other	Remaining unclassified grids (e.g., desert or tundra)

involved training the model with samples from specific years and testing it with data from years not used in training. For these two validation methods, the R^2 values for PM₁₀ were 0.83 and 0.41, with RMSE values of 29.99 and 55.44 µg m⁻³, respectively. For PM_{2.5}, the R^2 values were 0.83 and 0.52, with RMSE values of 16.46 and 28.11 µg m⁻³, respectively. The DOET model is relatively robust based on sample and spatial validation results.

By inputting TOAR, meteorological elements and geographical information into the optimally parameterized DOET model, a pollutant estimation dataset for eastern China was generated for the period September 2015 to August 2023. Due to the incomplete spatial coverage of TOAR data in different months and hours (Song et al., 2024), the study first calculated monthly averages, which were then used to derive annual averages. This step helps to minimize errors due to insufficient spatial coverage of the samples (Ding et al., 2024). As shown in Fig. 2a and b, the Beijing-Tianjin-Hebei region, the Sichuan Basin, the Guanzhong region, and central China are hotspots for PM₁₀ and PM_{2.5} pollution (Wei et al., 2021a), with concentrations reaching up to $100 \,\mu\mathrm{g}\,\mathrm{m}^{-3}$ for PM_{10} and $60 \,\mu\mathrm{g}\,\mathrm{m}^{-3}$ for $PM_{2.5}$. In addition, the Inner Mongolia region and northern Gansu, which are frequently affected by dust storms, are also characterized by high PM₁₀ concentrations (Li et al., 2012). Overall, the PM₁₀ and PM_{2.5} concentrations generated by the DOET model accurately reflect the spatial distribution characteristics of PM in eastern China, and the estimation results are consistent with those of previous studies (Yang et al., 2023; Chen et al., 2022b; Song et al., 2022a).

3.2 Urban-rural differences in PM pollution trends in recent years

The spatial distribution characteristics of PM_{10} and $PM_{2.5}$ trends from 2015 to 2023 were analysed, and the results (Fig. 3c–f) show a remarkable improvement of PM pollution in eastern China, as indicated by a significant decreasing trend in PM concentrations. The average decrease for PM_{10} was $-4.02 \pm 1.29 \,\mu g \, m^{-3} \, yr^{-1}$, while for $PM_{2.5}$, it was $-2.41 \pm 0.91 \,\mu g \, m^{-3} \, yr^{-1}$. However, this widespread decrease in PM concentrations showed considerable spa-

tial heterogeneity between urban and rural areas. The urban and rural decrease trends for PM_{10} were -4.99 ± 1.68 and $-3.98 \pm 1.26 \,\mu\text{g m}^{-3} \,\text{yr}^{-1}$, respectively, while for PM_{2.5}, they were -3.43 ± 1.10 and $-2.38 \pm 0.88 \,\mu \text{g m}^{-3} \,\text{yr}^{-1}$, respectively. This suggests that the decrease in PM concentrations in rural areas was close to the regional average in eastern China, while the decrease in urban areas was more pronounced than the overall trend. We supplemented our analysis by examining the relative change trends through benchmark concentration standardization. Initially, the standard deviation of PM concentrations was computed for each grid point to assess spatial variability. Subsequently, the annual mean PM data were used to calculate yearly relative changes normalized against benchmark concentrations. Finally, a comprehensive trend analysis was performed on these standardized values. The results are presented in Fig. S2. Consistent with the overall trends in PM concentrations, the relative change rates of PM_{2.5} were quantified as $-38.24 \pm 3.40 \% \text{ yr}^{-1}$ in rural areas and $-40.93 \pm 1.91 \% \text{ yr}^{-1}$ in urban areas. Similarly, PM₁₀ exhibited relative change trends of $-34.03 \pm 6.55 \% \text{ yr}^{-1}$ (rural) and $-39.07 \pm 2.78 \% \text{ yr}^{-1}$ (urban). These findings demonstrate that, when accounting for region-specific baseline concentrations across different land cover types, urban areas continue to show a more substantial reduction in PM pollution compared to rural areas.

From a broader perspective of the changes in particulate matter concentrations in eastern China, the urban decrease trends for PM_{10} and $PM_{2.5}$ were -0.47 and $-0.33\,\mu g\,m^{-3}$ per month, respectively, while the rural decrease trends were -0.37 and $-0.22\,\mu g\,m^{-3}$ per month, respectively. These results indicate that the reduction trend in rural areas was slower than in urban areas. By 2023, particulate matter concentrations in urban areas had decreased from about $20\,\mu g\,m^{-3}$ higher than in rural areas to levels almost equal to those in rural areas.

Urban and rural areas, categorized by land cover type, comprised eight different categories. The study assessed their respective roles in PM concentration reduction trends and found that all eight categories showed declining PM trends. However, the regions with the highest PM reduction trends were mainly four types: urban core areas, suburbs, towns

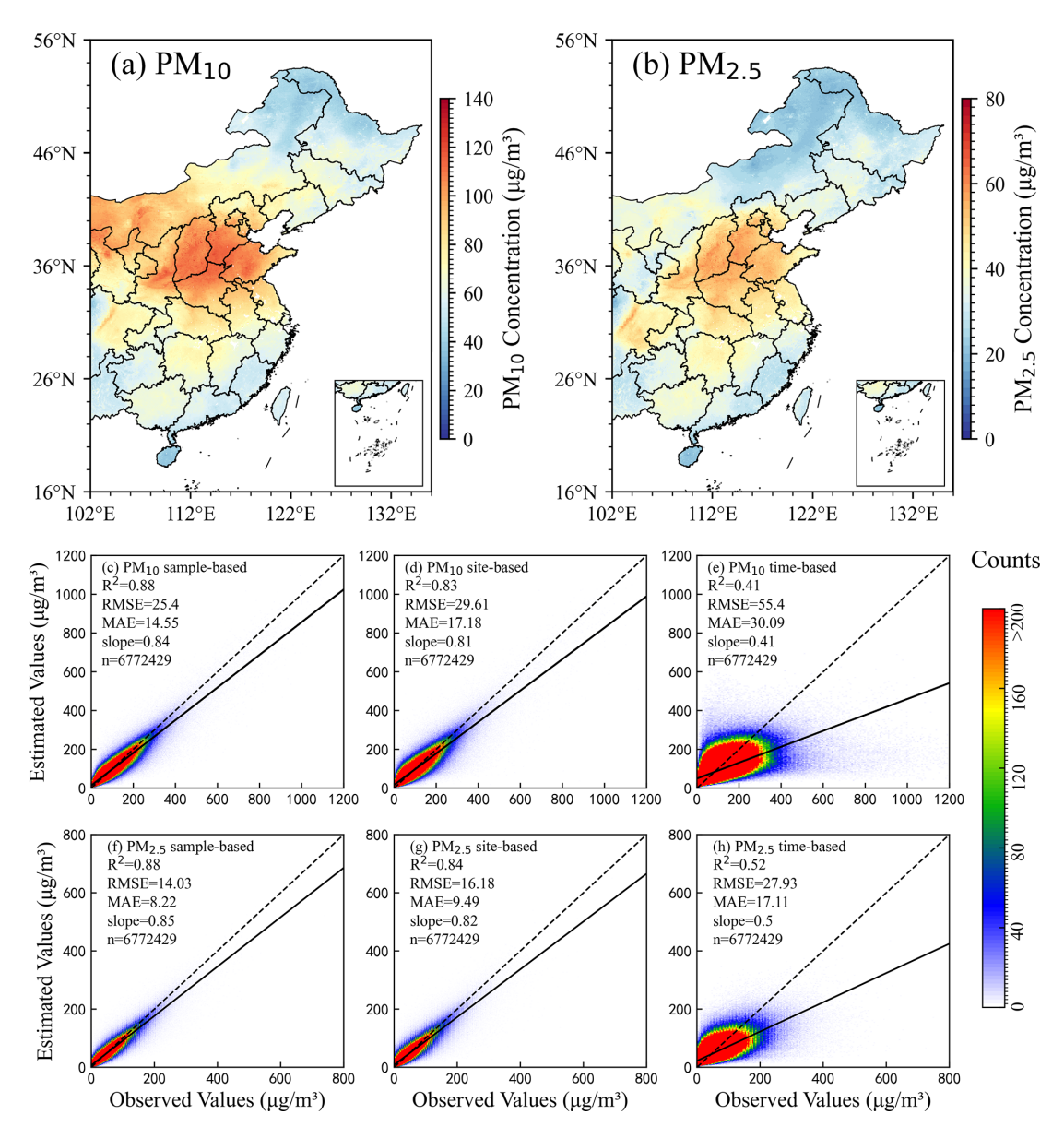


Figure 2. Spatial distribution of PM_{10} and $PM_{2.5}$ and cross validation results of the DOET model. The dashed lines represent the 1:1 line, while the solid lines show the fitted line between observed and estimated values.

and agricultural land 1 (high agricultural pressure). In contrast, the reduction trends were less pronounced in agricultural land 2 (low agricultural pressure), forests, grassland and other areas.

The trends in PM_{10} and $PM_{2.5}$ concentrations were categorized into four levels based on percentiles: slow decline (grid points with a decline trend below the 25th percentile), moderate decline (grid points with a decline trend between the 25th and 75th percentiles), rapid decline (grid points with a decline trend between the 75th and 95th percentiles), and sharp decline (grid points with a decline trend above the 95th percentile). As shown in Fig. 4, the regions with the most significant changes in urban and rural PM trends are

mainly concentrated in the Beijing-Tianjin-Hebei region, the Guanzhong region and Central China.

In areas with slow and moderate declines, forests and grasslands accounted for the highest proportions, ranging from 23.51% to 32.56% and 23.92% to 39.25%, respectively, followed by the agricultural 1 and agricultural 2, which accounted for about 20%. In regions with rapid decline, the first type of agricultural land had the highest proportion, ranging from 30% to 40%. Urban core, suburban and towns had higher proportions in the fast decline regions, accounting for 6.44%, 6.01% and 6.83% of the PM₁₀ decline trends and 7.52%, 6.34% and 7.21% of the PM_{2.5} de-

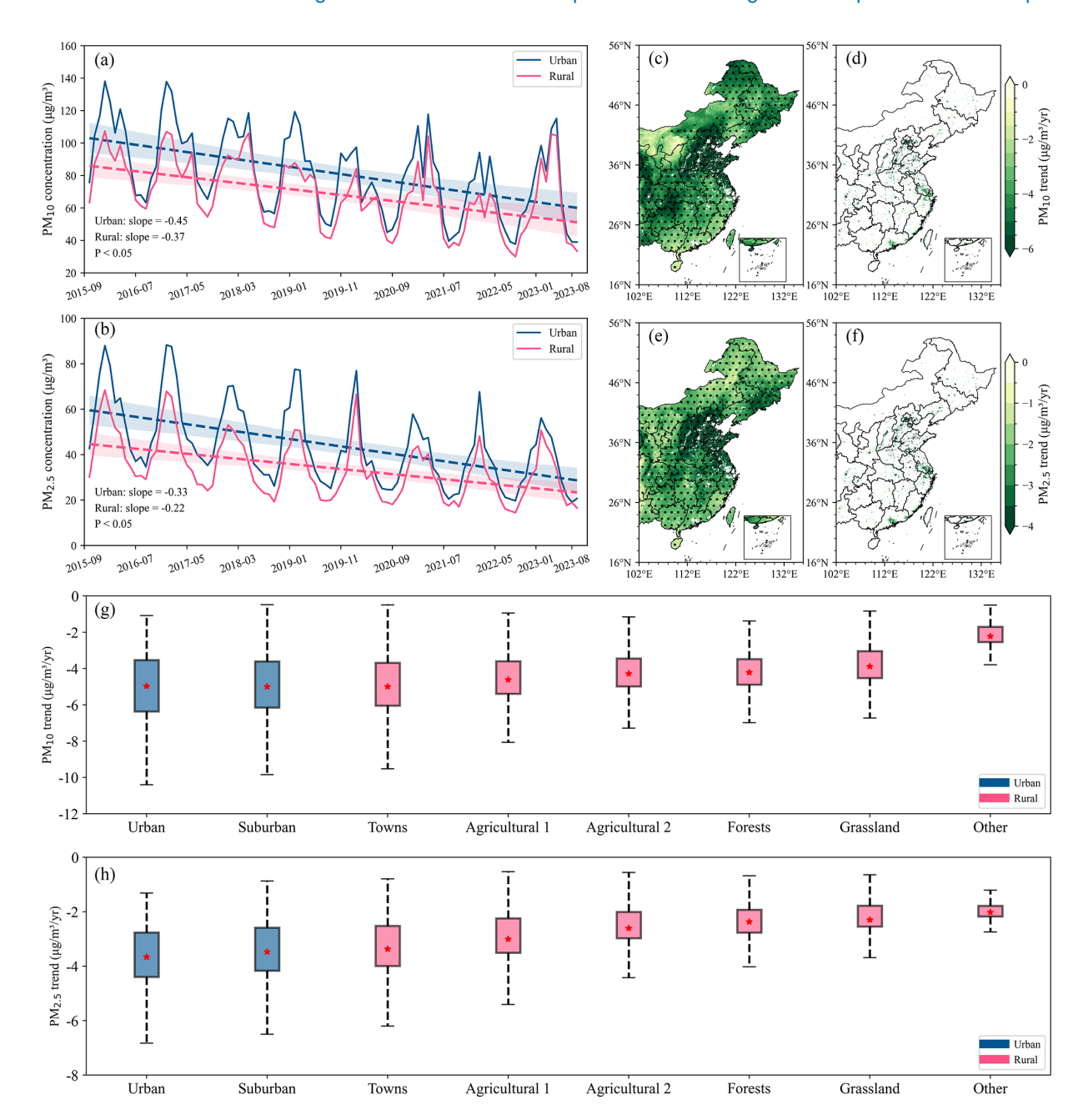


Figure 3. Analysis of PM concentration trends in eastern China from September 2015 to August 2023. Panels (a), (c), (d), and (g) represent PM_{10} , while panels (b), (e), (f), and (h) represent $PM_{2.5}$. In the legends of panels (g)–(h), blue indicates urban areas, and red indicates rural areas. In (g) and (h), the upper part of the box represents the upper quartile of the trend, and the lower part represents the lower quartile of the trend; the dotted line range represents the upper and lower limits of the trend values; the red dot represents the average value of the trend.

cline trends respectively. In particular, the agricultural 1 had the largest share in the strong decrease regions.

3.3 Assessing potential driving factors for PM pollution improvement and quantifying their contributions

A DOET model based on monthly PM data was developed to identify the key drivers of urban and rural particulate matter pollution changes in China. Monthly mean PM_{10} and $PM_{2.5}$

concentrations were correlated with meteorological factors and two temporal variables (year and month) representing the effects of meteorological changes and anthropogenic influences, respectively (see Methods for details). The model was cross-validated using a random training set (70 %) and a validation set (30 %). As shown in Fig. S3, the DOET model explains more than 60 % of the PM $_{10}$ trends and 80 % of the PM $_{2.5}$ trends in eastern China.

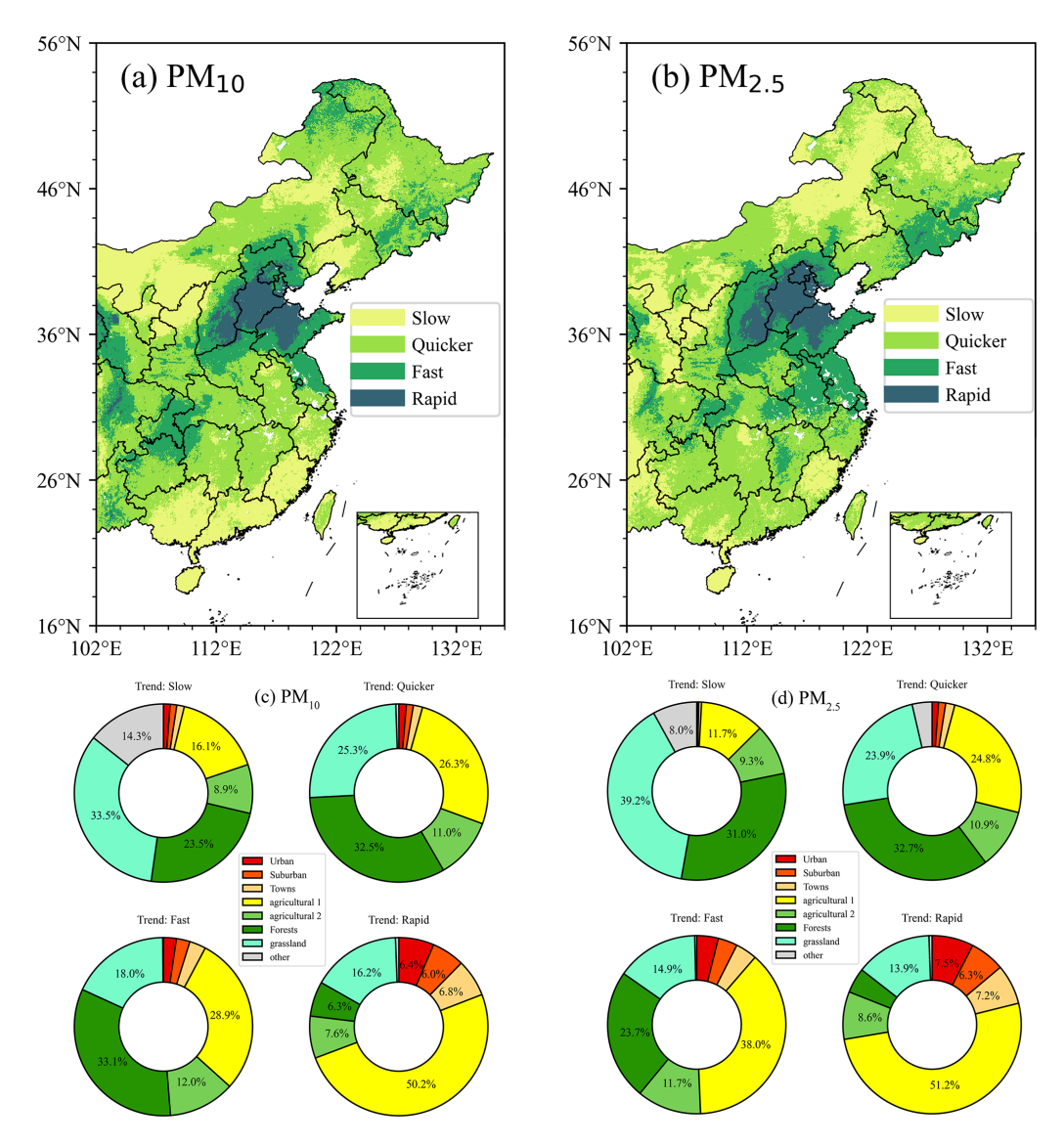


Figure 4. Spatial distribution of particulate matter trend percentiles and pie charts. The individual color scales in the figure represent different areas.

The relative importance of each variable in the DOET model was determined using the permutation_importance library. Inter-annual variability, intra-annual variability, air pressure and temperature were identified as significant contributors to the improvement of urban and rural PM pollution in eastern China (relative importance > 10 %). Among them, interannual variability was the most influential factor for PM $_{10}$ (26.14 \pm 13.35 %), followed by temperature (19.95 \pm 15.06 %) (Fig. 5a). In contrast, for PM $_{2.5}$, interannual variability ranked second (30.79 \pm 12.86 %), while temperature had a stronger effect (38.90 \pm 17.73 %) (Fig. 5b). The spatial distribution of the relative importance of the four main contributing factors, shown in Fig. 5c–r, indicates that regions with high relative importance values overlapped with PM pollution hotspots. Furthermore, as shown in Fig. S4, the

driving factors for urban and rural PM pollution improvement differed significantly between land cover types.

The relative contributions of each variable in the DOET model to the PM concentration values were obtained using the permutation_importance library. The results showed that the improvement in urban and rural PM pollution was primarily driven by interannual variation (Fig. 5), followed by temperature, which is consistent with the relative importance results in Fig. 5. Figures S5–S6 illustrate how variations in the values of the driving factors influence their relative contributions to PM concentrations. In particular, PM concentrations showed a clear inverse relationship with temperature and interannual variations, especially for PM_{2.5}. Relative humidity also showed clear differences in its contribution to PM₁₀ and PM_{2.5}: lower relative humidity was associ-

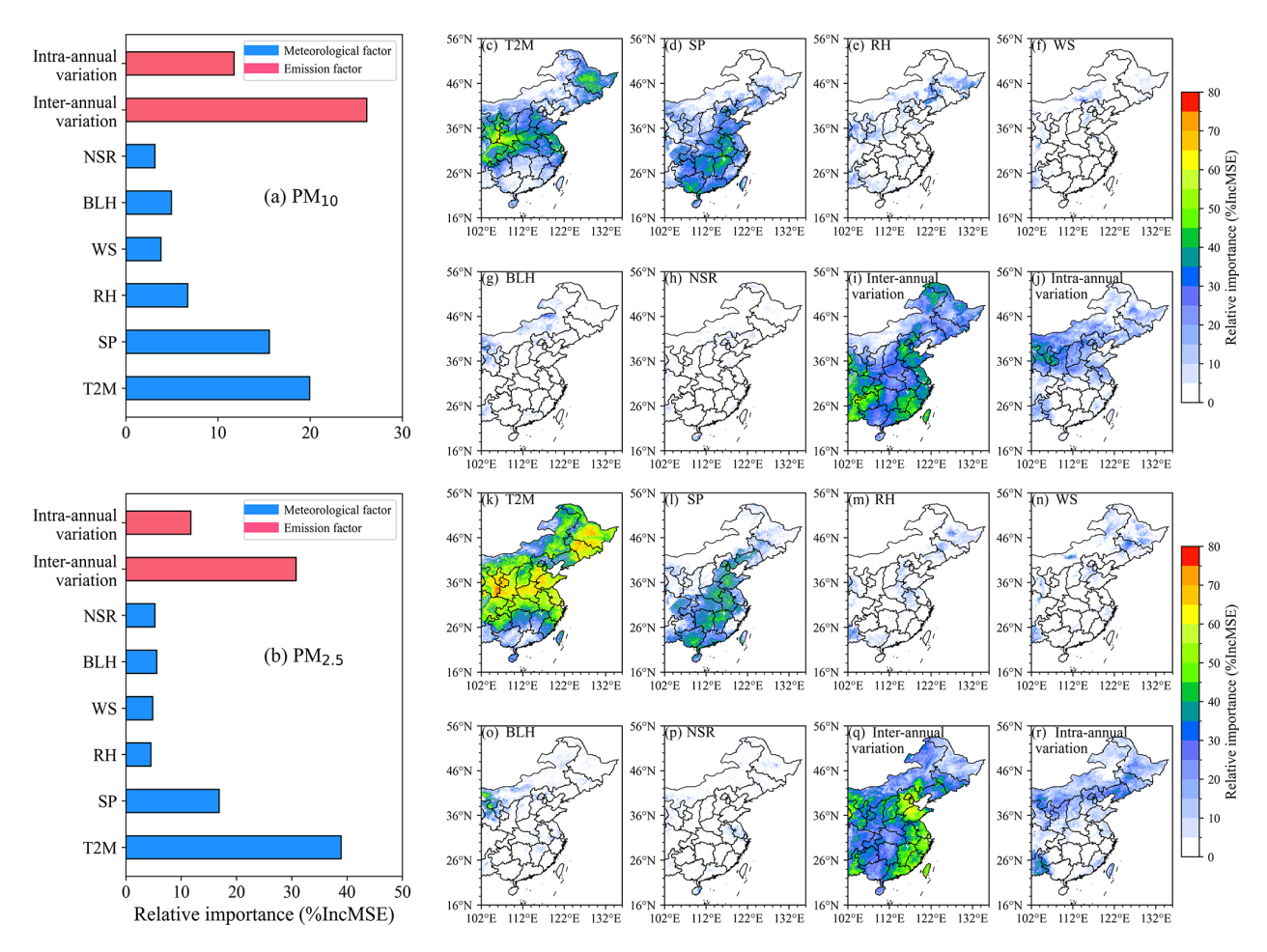


Figure 5. Spatial distribution of the relative influence of each variable on PM pollution. In panels (a)–(b), the red variables are related to emissions and the blue variables are related to meteorology.

ated with higher PM_{10} concentrations, whereas higher $PM_{2.5}$ concentrations were associated with higher relative humidity. The scatter plots illustrating the relationships between other variables and their relative contributions to PM are shown in Figs. S4–S5.

Figure 6 shows the relative contributions of each variable, with the spatial distribution patterns of interannual variations being particularly noteworthy. For PM₁₀, regions such as Guanzhong, North China, and Inner Mongolia were more susceptible to the influence of interannual variations. We hypothesize that the improvement in PM₁₀ pollution be due not only be attributed to anthropogenic emission reductions but also to sandstorm events in recent years, which are important sources of PM₁₀ (Wang et al., 2024c). However, the explanatory power of the model for PM₁₀ trends in these areas remains relatively low, suggesting the need for further investigation into the specific causes. For PM_{2.5}, the impact of interannual variability was observed mainly in the Guanzhong region, North China, and the Sichuan Basin, all of which are key areas for pollution control (Wang et al., 2022a; Yu et al., 2022). Contrary to the relative importance results, the dominant factor driving the improvement in urban and rural PM pollution was the influence of interannual variability (Fig. S7), with other variables showing varying effects across different land cover types.

Finally, the "tree_SHAP" tool was used to decompose the SHAP values of each variable in the DOET model. By analyzing the positive and negative changes in the SHAP values, the influence of each variable on the PM pollution improvement – whether positive or negative – was quantified, thus complementing the assessment of driving factor contributions (Li et al., 2024a). As shown in Fig. 7, the SHAP values show a strong negative correlation between PM concentrations and the contribution of interannual variability in eastern China. In particular, during the transition from 2019 to 2020, the contribution of interannual variations to PM concentrations shifted critically from positive to negative. Interestingly, despite the high relative importance and contribution of some variables, their SHAP values showed periodic fluctuations, alternating between positive and negative, such as for temperature (with a negative contribution in summer and a positive one in winter). This suggests that mete-

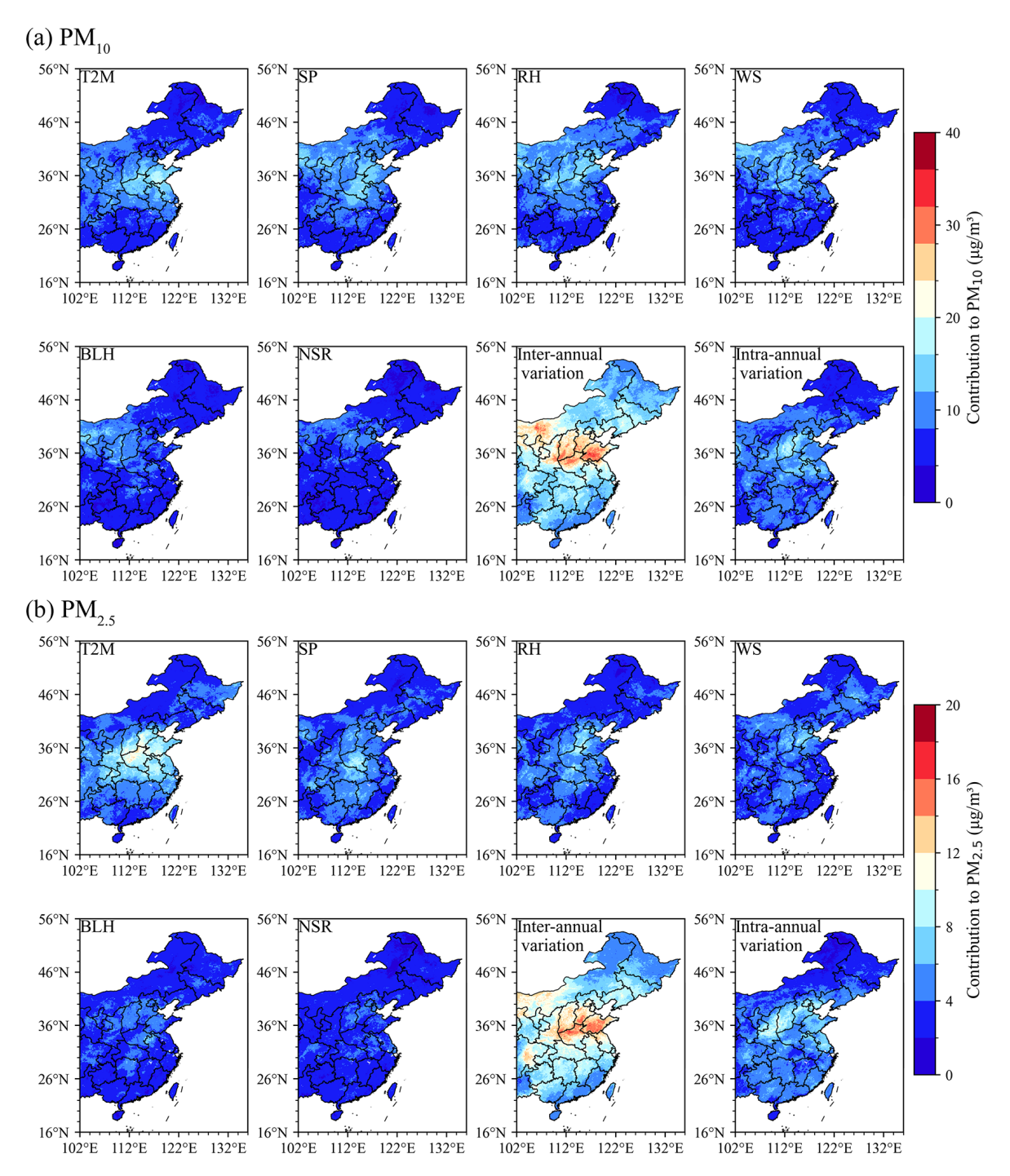


Figure 6. The spatial distribution of the relative contributions of each variable to PM pollution.

orological factors influence PM concentrations in a periodic manner, while the only factor that consistently contributes to the improvement of PM pollution is the interannual variation driven by anthropogenic influences. The Figs. S8–S9 show the SHAP values of various variables for PM in urban and rural areas, respectively. The impact of various variables, including temperature, on PM is primarily evident in urban ar-

eas, where the magnitude of the values and the rate of change are both higher than in rural areas.

3.4 Trends in the contribution of driving factors to PM pollution improvement

To further investigate the influence of potential driving factors on PM concentrations, we conducted a detailed analy-

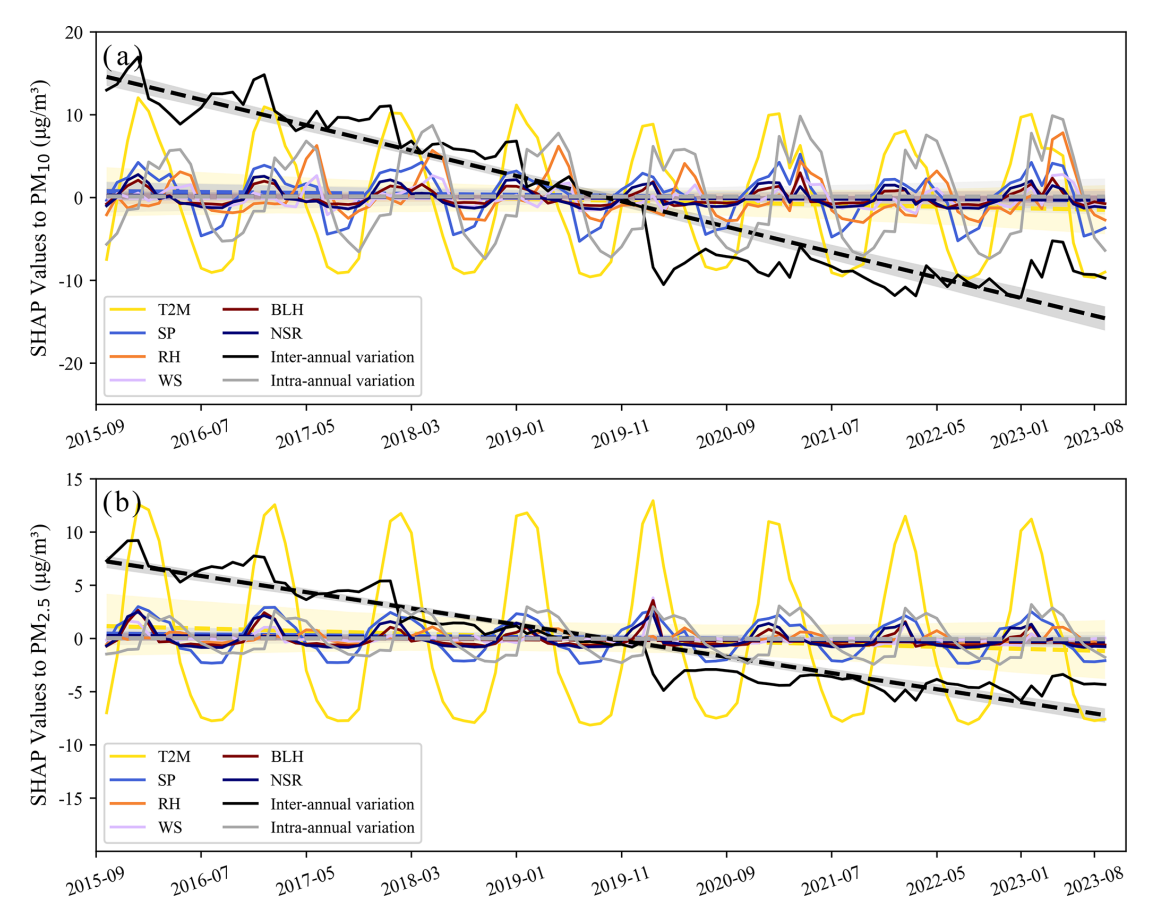


Figure 7. The SHAP values of each variable for PM. The solid line represents the SHAP values, and the dashed line indicates their trend of change.

sis of the trends in the contributions of each variable was performed. As shown in Figs. S10-S13, the monthly trends in the relative contributions and SHAP values of each variable were examined, categorized into significant changes (p < 0.05) and non-significant changes (p > 0.05). For the relative contributions (including PM₁₀ and PM_{2.5}), with the exception of interannual variations, all other variables showed a decreasing trend, although some regions showed an increasing trend. However, the contribution of interannual variability showed a significant decrease, indicating a reduced capacity of anthropogenic emissions to trigger PM pollution events. This phenomenon is more pronounced for the trends in SHAP values. In particular, only the contribution of interannual variations showed a significant decreasing trend, while the other variables showed non-significant decreasing trends, mainly due to the periodic variations in their contributions, as shown in Fig. 7. This shows that the impact of a variable on PM pollution cannot only be assessed on the basis of its relative contribution, but its positive or negative influence on the improvement of PM pollution must also be considered.

Given the significant decrease in the contribution of interannual variation, we further compared its trends across different land cover types in urban and rural areas, as this variable plays the most important role in PM pollution improvement. As shown in Fig. 8a-b, the trends in relative contributions for both PM₁₀ and PM_{2.5} did not differ significantly between the eight land cover types, although urban areas showed the highest rate of decrease. However, the trends in SHAP values shown in Fig. 8c-d revealed that the reduction in the contribution of interannual variation was most pronounced in urban core areas, suburban areas, and towns. In contrast, the decrease in interannual contributions was more pronounced in agricultural areas than in urban areas, while other rural areas showed a weaker influence of interannual variations on PM pollution improvement. These results suggest that the improvement in PM pollution in urban areas is more closely related to anthropogenic influences, whereas this relationship is less pronounced in rural areas.

4 Discussion and conclusion

Due to the predominant distribution of environmental quality monitoring stations in urban areas (Park et al., 2020), discussions on air pollution patterns between urban and ru-

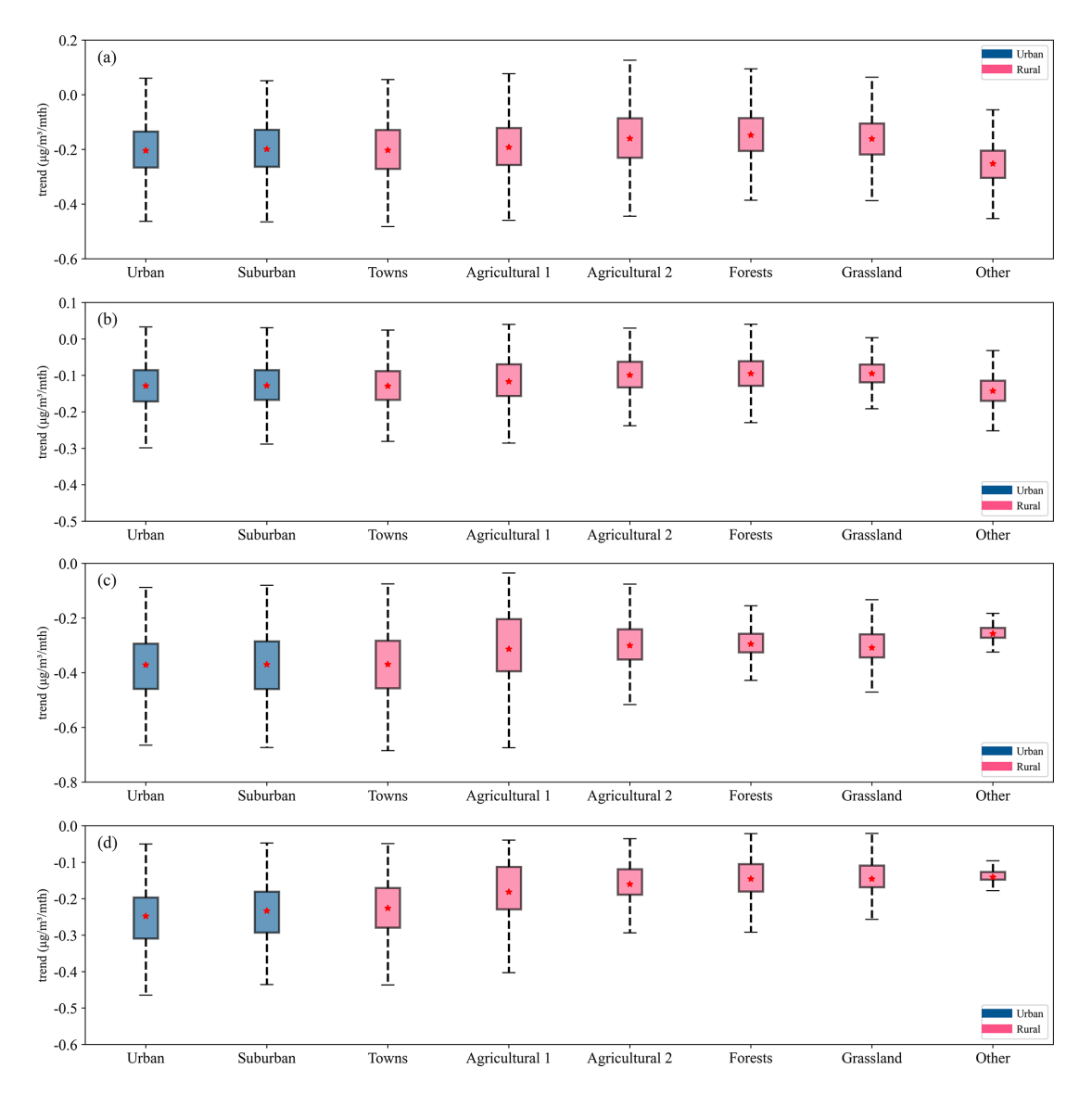


Figure 8. Trends in the relative contribution (\mathbf{a} - \mathbf{b}) and SHAP values (\mathbf{c} - \mathbf{d}) of interannual variability of different land cover types. (\mathbf{a}) and (\mathbf{c}) represent the case for PM₁₀, while (\mathbf{b}) and (\mathbf{d}) represent the case for PM_{2.5}. In the legend, blue represents urban areas, and red represents rural areas. In Fig. 8, the upper part of the box represents the upper quartile of the trend, and the lower part represents the lower quartile of the trend; the dotted line range represents the upper and lower limits of the trend values; the red dot represents the average value of the trend.

ral regions have been limited (Hammer et al., 2020). In this study, we used a regression-based machine learning DOET algorithm to integrate station-observed PM concentrations, satellite-observed TOAR, meteorological factors, and geographic information data. This approach enabled us to generate long-term, high spatio-temporal resolution datasets of near-surface PM $_{10}$ and PM $_{2.5}$, with a spatial resolution of 5 km, an hourly temporal resolution, and coverage across the entire eastern China region. Using the generated PM data in conjunction with a constructed urban-rural land type framework, we successfully captured the broad trends and patterns of PM $_{10}$ and PM $_{2.5}$ concentration changes from urban and suburban areas to different types of rural regions.

Based on the estimated dataset and interpretable parameters, the study identified significant large-scale improvements in PM pollution in eastern China from 2015 to 2023, indicating notable achievements from the implementation of clean air measures. The study noted that the second phase of the clean air action plan, implemented from 2018 to 2020, also produced positive results, following the success of the first phase from 2013 to 2017 (Geng et al., 2024). Our results show that under the urban-rural framework, PM reductions are generally higher in urban areas than in rural areas. However, the highly polluted agricultural areas in rural regions also showed significant improvements in PM pollution. In fact, during air pollution prevention and control efforts,

China's main emission reduction measures focused on coal consumption and energy-intensive industries such as steel and cement, and these measures were often effective in urban areas (Yun et al., 2020; Huang et al., 2014b; Wang et al., 2013). This does not mean that rural areas have been neglected, as evidenced by reductions in biomass burning (Shen et al., 2019). The finding that interannual variability is the main driver of PM pollution improvement is consistent with these facts. It is worth noting that the rate of PM concentration decline is faster in urban areas than in rural areas, bringing the concentration levels of the two areas closer together. Given the more pronounced decrease in the contribution of inter-annual variations in urban areas, future efforts to prevent and control air pollution should maintain the current intensity or balance investments between urban and rural areas.

Our results indicate that meteorological factors with distinct seasonal variations, such as temperature, boundary layer height, and relative humidity, have a cyclical influence on PM pollution. For example, summer weather conditions, such as abundant precipitation, high relative humidity and abundant water vapour favour PM dispersion, while winter weather conditions are less conducive to pollutant dispersion and spring is often characterised by frequent dust events. Therefore, due to their periodic positive and negative contributions and variability, meteorological conditions do not provide stable improvements in PM pollution. Moreover, the contribution of meteorological conditions to PM concentrations does not show a significant trend. Thus, given the high contribution of inter-annual variability to the improvement of PM pollution, the impact of meteorological conditions on the inter-annual variability of PM pollution in China should not be overemphasised.

Although this study evaluated the patterns of PM pollution improvement and its driving factors in urban and rural areas of eastern China, the contribution of interannual variations driven by anthropogenic influences was represented by a time variable in our analysis. In the future, key factors driving changes in air pollutants, such as energy management, urban traffic management, agricultural nitrogen deposition effects and biomass burning, need to be further incorporated into the attribution analysis to distinguish and quantify the contributions of different anthropogenic emission reduction measures to PM pollution improvement. Given the different drivers of PM pollution improvement in urban and rural areas, it is essential to implement tailored strategies in both regions to achieve more effective and comprehensive air pollution prevention and control measures in the future.

Code availability. The codes are available from the corresponding author upon request.

Data availability. The hourly ground station observations of near-surface PM₁₀ and PM_{2.5} concentrations are obtained from the China National Environmental Monitoring Center (CNEMC), which can be accessed on its official website (http://www.cnemc.cn/en/, CNEMC, 2025). Himawari-8 TOAR data provided by the Japan Meteorological Agency (http://www.eorc.jaxa.jp/ptree/index.html, last access: 20 September 2025). Meteorological variables were derived from the reanalysis data set provided by the European Centre for Medium-Range Weather Forecasts (ECMWF) (https://cds.climate.copernicus.eu/cdsapp#!/dataset/, 2025). MODIS Land use/cover change (LUCC) product can be downloaded from https://doi.org/10.5067/MODIS/MCD12C1.061 (Friedl and Sulla-Menashe, 2022). The 2015 UN-adjusted population density data (RK) can be downloaded from http: //sedac.ciesin.columbia.edu/data/collection/gpw-v4/documentation (Center For International Earth Science Information Network-CIESIN-Columbia University, 2018). SRTM-3 elevation data jointly measured by NASA and the U.S. Department of Defense's National Imagery and Mapping Agency (NIMA) (HEIGHT) can be downloaded from https://doi.org/10.5067/MEaSUREs/SRTM/SRTMGL3.003 (NASA JPL, 2013). The particulate matter data generated in the manuscript can be obtained at the following URL: https://doi.org/10.5281/zenodo.17090707 (Song, 2025).

Supplement. The supplement related to this article is available online at https://doi.org/10.5194/acp-25-15487-2025-supplement.

Author contributions. ZS: Software, Methodology, Data curation, Writing – Original draft preparation, Formal Analysis, Visualization. BC: Conceptualization, Methodology, Writing – Reviewing and Editing, Resources.

Competing interests. The contact author has declared that neither of the authors has any competing interests.

Disclaimer. Publisher's note: Copernicus Publications remains neutral with regard to jurisdictional claims made in the text, published maps, institutional affiliations, or any other geographical representation in this paper. While Copernicus Publications makes every effort to include appropriate place names, the final responsibility lies with the authors. Views expressed in the text are those of the authors and do not necessarily reflect the views of the publisher.

Acknowledgements. We would like to express our gratitude to the China National Environmental Monitoring Center, Japan Meteorological Agency, European Centre for Medium-Range Weather Forecasts, and NASA for their datasets. The study supported by Supercomputing Center of Lanzhou University.

Financial support. The work was supported by the Noncommunicable Chronic Diseases-National Science and Technology Major Project (grant no. 2024ZD0531600), the National Natural Science Foundation of China (grant no. 42427803), the Gansu Provincial Science and Technology Plan (grant no. 25RCKA024), and the Fundamental Research Funds for the Central Universities (grant no. lzujbky-2023-ey10).

Review statement. This paper was edited by Qi Chen and reviewed by three anonymous referees.

References

- An, Z., Huang, R.-J., Zhang, R., Tie, X., Li, G., Cao, J., Zhou, W., Shi, Z., Han, Y., Gu, Z., and Ji, Y.: Severe haze in northern China: A synergy of anthropogenic emissions and atmospheric processes, Proceedings of the National Academy of Sciences, 116, 8657–8666, https://doi.org/10.1073/pnas.1900125116, 2019.
- Apte, J. S., Marshall, J. D., Cohen, A. J., and Brauer, M.: Addressing Global Mortality from Ambient PM_{2.5}, Environmental Science & Technology, 49, 8057–8066, https://doi.org/10.1021/acs.est.5b01236, 2015.
- Berner, L. T., Massey, R., Jantz, P., Forbes, B. C., Macias-Fauria, M., Myers-Smith, I., Kumpula, T., Gauthier, G., Andreu-Hayles, L., Gaglioti, B. V., Burns, P., Zetterberg, P., D'Arrigo, R., and Goetz, S. J.: Summer warming explains widespread but not uniform greening in the Arctic tundra biome, Nature Communications, 11, 4621, https://doi.org/10.1038/s41467-020-18479-5, 2020.
- Bessho, K., Date, K., Hayashi, M., Ikeda, A., Imai, T., Inoue, H., Kumagai, Y., Miyakawa, T., Murata, H., Ohno, T., Okuyama, A., Oyama, R., Sasaki, Y., Shimazu, Y., Shimoji, K., Sumida, Y., Suzuki, M., Taniguchi, H., Tsuchiyama, H., Uesawa, D., Yokota, H., and Yoshida, R.: An Introduction to Himawari-8/9 Japan's New-Generation Geostationary Meteorological Satellites, Journal of the Meteorological Society of Japan Ser. II, 94, 151–183, https://doi.org/10.2151/jmsj.2016-009, 2016.
- Brauer, M., Freedman, G., Frostad, J., van Donkelaar, A., Martin, R. V., Dentener, F., Dingenen, R. V., Estep, K., Amini, H., Apte, J. S., Balakrishnan, K., Barregard, L., Broday, D., Feigin, V., Ghosh, S., Hopke, P. K., Knibbs, L. D., Kokubo, Y., Liu, Y., Ma, S., Morawska, L., Sangrador, J. L. T., Shaddick, G., Anderson, H. R., Vos, T., Forouzanfar, M. H., Burnett, R. T., and Cohen, A.: Ambient Air Pollution Exposure Estimation for the Global Burden of Disease 2013, Environmental Science & Technology, 50, 79–88, https://doi.org/10.1021/acs.est.5b03709, 2016.
- Burnett, R., Chen, H., Szyszkowicz, M., Fann, N., Hubbell, B.,
 Pope, C. A., Apte, J. S., Brauer, M., Cohen, A., Weichenthal,
 S., Coggins, J., Di, Q., Brunekreef, B., Frostad, J., Lim, S. S.,
 Kan, H., Walker, K. D., Thurston, G. D., Hayes, R. B., Lim,
 C. C., Turner, M. C., Jerrett, M., Krewski, D., Gapstur, S. M.,
 Diver, W. R., Ostro, B., Goldberg, D., Crouse, D. L., Martin, R.
 V., Peters, P., Pinault, L., Tjepkema, M., van Donkelaar, A., Villeneuve, P. J., Miller, A. B., Yin, P., Zhou, M., Wang, L., Janssen,
 N. A. H., Marra, M., Atkinson, R. W., Tsang, H., Quoc Thach,
 T., Cannon, J. B., Allen, R. T., Hart, J. E., Laden, F., Cesaroni,
 G., Forastiere, F., Weinmayr, G., Jaensch, A., Nagel, G., Concin,

- H., and Spadaro, J. V.: Global estimates of mortality associated with long-term exposure to outdoor fine particulate matter, Proceedings of the National Academy of Sciences, 115, 9592–9597, https://doi.org/10.1073/pnas.1803222115, 2018.
- Burnett Richard, T., Pope, C. A., Ezzati, M., Olives, C., Lim Stephen, S., Mehta, S., Shin Hwashin, H., Singh, G., Hubbell, B., Brauer, M., Anderson, H. R., Smith Kirk, R., Balmes John, R., Bruce Nigel, G., Kan, H., Laden, F., Prüss-Ustün, A., Turner Michelle, C., Gapstur Susan, M., Diver, W. R., and Cohen, A.: An Integrated Risk Function for Estimating the Global Burden of Disease Attributable to Ambient Fine Particulate Matter Exposure, Environmental Health Perspectives, 122, 397-403, https://doi.org/10.1289/ehp.1307049, 2014.
- Cao, B. and Yin, Z.: Future atmospheric circulations benefit ozone pollution control in Beijing-Tianjin-Hebei with global warming, Science of The Total Environment, 743, 140645, https://doi.org/10.1016/j.scitotenv.2020.140645, 2020.
- Center For International Earth Science Information Network-CIESIN-Columbia University: Gridded Population of the World, Version 4 (GPWv4): Population Count Adjusted to Match 2015 Revision of UN WPP Country Totals, Revision 11 (Version 4.11), Palisades, NY, NASA Socioeconomic Data and Applications Center (SEDAC) [data set], https://doi.org/10.7927/H4PN93PB, 2018.
- Chen, B., Hu, J., and Wang, Y.: Synergistic observation of FY-4A&4B to estimate CO concentration in China: combining interpretable machine learning to reveal the influencing mechanisms of CO variations, npj Climate and Atmospheric Science, 7, 9, https://doi.org/10.1038/s41612-023-00559-0, 2024a.
- Chen, B., Song, Z., Pan, F., and Huang, Y.: Obtaining vertical distribution of PM_{2.5} from CALIOP data and machine learning algorithms, Science of The Total Environment, 805, 150338, https://doi.org/10.1016/j.scitotenv.2021.150338, 2022a.
- Chen, B., Song, Z., Shi, B., and Li, M.: An interpretable deep forest model for estimating hourly PM₁₀ concentration in China using Himawari-8 data, Atmospheric Environment, 268, 118827, https://doi.org/10.1016/j.atmosenv.2021.118827, 2022b.
- Chen, B., Wang, Y., Huang, J., Zhao, L., Chen, R., Song, Z., and Hu, J.: Estimation of near-surface ozone concentration and analysis of main weather situation in China based on machine learning model and Himawari-8 TOAR data, Science of The Total Environment, 864, 160928, https://doi.org/10.1016/j.scitotenv.2022.160928, 2023.
- Chen, B., Song, Z., Huang, J., Zhang, P., Hu, X., Zhang, X., Guan, X., Ge, J., and Zhou, X.: Estimation of Atmospheric PM₁₀ Concentration in China Using an Interpretable Deep Learning Model and Top-of-the-Atmosphere Reflectance Data From China's New Generation Geostationary Meteorological Satellite, FY-4A, Journal of Geophysical Research: Atmospheres, 127, e2021JD036393, https://doi.org/10.1029/2021JD036393, 2022c.
- Chen, C.-C., Wang, Y.-R., Yeh, H.-Y., Lin, T.-H., Huang, C.-S., and Wu, C.-F.: Estimating monthly PM_{2.5} concentrations from satellite remote sensing data, meteorological variables, and land use data using ensemble statistical modeling and a random forest approach, Environmental Pollution, 291, 118159, https://doi.org/10.1016/j.envpol.2021.118159, 2021.
- Chen, G., Li, S., Knibbs, L. D., Hamm, N. A. S., Cao, W., Li, T., Guo, J., Ren, H., Abramson, M. J., and Guo, Y.: A machine learning method to estimate PM_{2.5} concentrations across

- China with remote sensing, meteorological and land use information, Science of The Total Environment, 636, 52–60, https://doi.org/10.1016/j.scitotenv.2018.04.251, 2018a.
- Chen, J., Yin, J., Zang, L., Zhang, T., and Zhao, M.: Stacking machine learning model for estimating hourly PM_{2.5} in China based on Himawari 8 aerosol optical depth data, Science of The Total Environment, 697, 134021, https://doi.org/10.1016/j.scitotenv.2019.134021, 2019a.
- Chen, J., Li, Z., Lv, M., Wang, Y., Wang, W., Zhang, Y., Wang, H., Yan, X., Sun, Y., and Cribb, M.: Aerosol hygroscopic growth, contributing factors, and impact on haze events in a severely polluted region in northern China, Atmos. Chem. Phys., 19, 1327– 1342, https://doi.org/10.5194/acp-19-1327-2019, 2019b.
- Chen, L., Zhu, J., Liao, H., Yang, Y., and Yue, X.: Meteorological influences on PM_{2.5} and O₃ trends and associated health burden since China's clean air actions, Science of The Total Environment, 744, 140837, https://doi.org/10.1016/j.scitotenv.2020.140837, 2020a.
- Chen, S., Guo, J., Song, L., Li, J., Liu, L., and Cohen, J. B.: Interannual variation of the spring haze pollution over the North China Plain: Roles of atmospheric circulation and sea surface temperature, International Journal of Climatology, 39, 783–798, https://doi.org/10.1002/joc.5842, 2019c.
- Chen, X., Zhang, W., He, J., Zhang, L., Guo, H., Li, J., and Gu, X.: Mapping PM_{2.5} concentration from the top-of-atmosphere reflectance of Himawari-8 via an ensemble stacking model, Atmospheric Environment, 330, 120560, https://doi.org/10.1016/j.atmosenv.2024.120560, 2024b.
- Chen, Z., Xie, X., Cai, J., Chen, D., Gao, B., He, B., Cheng, N., and Xu, B.: Understanding meteorological influences on PM_{2.5} concentrations across China: a temporal and spatial perspective, Atmos. Chem. Phys., 18, 5343–5358, https://doi.org/10.5194/acp-18-5343-2018, 2018b.
- Chen, Z., Chen, D., Zhao, C., Kwan, M.-p., Cai, J., Zhuang, Y., Zhao, B., Wang, X., Chen, B., Yang, J., Li, R., He, B., Gao, B., Wang, K., and Xu, B.: Influence of meteorological conditions on PM_{2.5} concentrations across China: A review of methodology and mechanism, Environment International, 139, 105558, https://doi.org/10.1016/j.envint.2020.105558, 2020b.
- Cheng, J., Tong, D., Zhang, Q., Liu, Y., Lei, Y., Yan, G., Yan, L., Yu, S., Cui, R. Y., Clarke, L., Geng, G., Zheng, B., Zhang, X., Davis, S. J., and He, K.: Pathways of China's PM_{2.5} air quality 2015–2060 in the context of carbon neutrality, National Science Review, 8, nwab078, https://doi.org/10.1093/nsr/nwab078, 2021.
- CNEMC: ground-based PM, CNEMC [data set], http://www.cnemc.cn, last access: 20 September 2025.
- Cohen, A. J., Brauer, M., Burnett, R., Anderson, H. R., Frostad, J., Estep, K., Balakrishnan, K., Brunekreef, B., Dandona, L., Dandona, R., Feigin, V., Freedman, G., Hubbell, B., Jobling, A., Kan, H., Knibbs, L., Liu, Y., Martin, R., Morawska, L., Pope, C. A., Shin, H., Straif, K., Shaddick, G., Thomas, M., van Dingenen, R., van Donkelaar, A., Vos, T., Murray, C. J. L., and Forouzanfar, M. H.: Estimates and 25-year trends of the global burden of disease attributable to ambient air pollution: an analysis of data from the Global Burden of Diseases Study 2015, The Lancet, 389, 1907–1918, https://doi.org/10.1016/S0140-6736(17)30505-6, 2017.
- Dai, Q., Hou, L., Liu, B., Zhang, Y., Song, C., Shi, Z., Hopke, P. K., and Feng, Y.: Spring Festival and COVID-19 Lockdown: Disentangling PM Sources in Major Chinese

- Cities, Geophysical Research Letters, 48, e2021GL093403, https://doi.org/10.1029/2021GL093403, 2021.
- Ding, Y., Li, S., Xing, J., Li, X., Ma, X., Song, G., Teng, M., Yang, J., Dong, J., and Meng, S.: Retrieving hourly seamless PM_{2.5} concentration across China with physically informed spatiotemporal connection, Remote Sensing of Environment, 301, 113901, https://doi.org/10.1016/j.rse.2023.113901, 2024.
- ECMWF: ERA5, ECMWF [data set], https://cds.climate.copernicus.eu/cdsapp#!/dataset/, last access: 20 September 2025.
- Friedl, M. and Sulla-Menashe, D.: MODIS/Terra+Aqua Land Cover Type Yearly L3 Global 0.05Deg CMG V061, NASA Land Processes Distributed Active Archive Center [data set], https://doi.org/10.5067/MODIS/MCD12C1.061, 2022.
- Geng, G., Xiao, Q., Zheng, Y., Tong, D., Zhang, Y., Zhang, X., Zhang, Q., He, K., and Liu, Y.: Impact of China's Air Pollution Prevention and Control Action Plan on PM_{2.5} chemical composition over eastern China, Science China Earth Sciences, 62, 1872–1884, https://doi.org/10.1007/s11430-018-9353-x, 2019.
- Geng, G., Liu, Y., Liu, Y., Liu, S., Cheng, J., Yan, L., Wu, N., Hu, H., Tong, D., Zheng, B., Yin, Z., He, K., and Zhang, Q.: Efficacy of China's clean air actions to tackle PM_{2.5} pollution between 2013 and 2020, Nature Geoscience, 17, 987–994, https://doi.org/10.1038/s41561-024-01540-z, 2024.
- Geng, G., Xiao, Q., Liu, S., Liu, X., Cheng, J., Zheng, Y., Xue, T., Tong, D., Zheng, B., Peng, Y., Huang, X., He, K., and Zhang, Q.: Tracking Air Pollution in China: Near Real-Time PM_{2.5} Retrievals from Multisource Data Fusion, Environmental Science & Technology, 55, 12106–12115, https://doi.org/10.1021/acs.est.1c01863, 2021.
- Geurts, P., Ernst, D., and Wehenkel, L.: Extremely randomized trees, Machine Learning, 63, 3-42, https://doi.org/10.1007/s10994-006-6226-1, 2006.
- Grange, S. K. and Carslaw, D. C.: Using meteorological normalisation to detect interventions in air quality time series, Science of The Total Environment, 653, 578-588, https://doi.org/10.1016/j.scitotenv.2018.10.344, 2019.
- Gui, K., Che, H., Wang, Y., Wang, H., Zhang, L., Zhao, H., Zheng, Y., Sun, T., and Zhang, X.: Satellite-derived PM_{2.5} concentration trends over Eastern China from 1998 to 2016: Relationships to emissions and meteorological parameters, Environmental Pollution, 247, 1125–1133, https://doi.org/10.1016/j.envpol.2019.01.056, 2019.
- Hammer, M. S., van Donkelaar, A., Li, C., Lyapustin, A., Sayer,
 A. M., Hsu, N. C., Levy, R. C., Garay, M. J., Kalashnikova, O.
 V., Kahn, R. A., Brauer, M., Apte, J. S., Henze, D. K., Zhang,
 L., Zhang, Q., Ford, B., Pierce, J. R., and Martin, R. V.: Global
 Estimates and Long-Term Trends of Fine Particulate Matter Concentrations (1998–2018), Environmental Science & Technology,
 54, 7879–7890, https://doi.org/10.1021/acs.est.0c01764, 2020.
- He, J., Gong, S., Yu, Y., Yu, L., Wu, L., Mao, H., Song, C., Zhao, S., Liu, H., Li, X., and Li, R.: Air pollution characteristics and their relation to meteorological conditions during 2014–2015 in major Chinese cities, Environmental Pollution, 223, 484–496, https://doi.org/10.1016/j.envpol.2017.01.050, 2017.
- He, Q., Cao, J., Saide, P. E., Ye, T., and Wang, W.: Unraveling the Influence of Satellite-Observed Land Surface Temperature on High-Resolution Mapping of Ground-Level Ozone Using Interpretable Machine Learning, Environmental Science & Technol-

- ogy, 58, 15938–15948, https://doi.org/10.1021/acs.est.4c02926, 2024.
- Hersbach, H., Bell, B., Berrisford, P., Hirahara, S., Horányi, A., Muñoz-Sabater, J., Nicolas, J., Peubey, C., Radu, R., Schepers, D., Simmons, A., Soci, C., Abdalla, S., Abellan, X., Balsamo, G., Bechtold, P., Biavati, G., Bidlot, J., Bonavita, M., De Chiara, G., Dahlgren, P., Dee, D., Diamantakis, M., Dragani, R., Flemming, J., Forbes, R., Fuentes, M., Geer, A., Haimberger, L., Healy, S., Hogan, R. J., Hólm, E., Janisková, M., Keeley, S., Laloyaux, P., Lopez, P., Lupu, C., Radnoti, G., de Rosnay, P., Rozum, I., Vamborg, F., Villaume, S., and Thépaut, J.-N.: The ERA5 global reanalysis, Quarterly Journal of the Royal Meteorological Society, 146, 1999–2049, https://doi.org/10.1002/qj.3803, 2020.
- Hou, L., Dai, Q., Song, C., Liu, B., Guo, F., Dai, T., Li, L., Liu, B., Bi, X., Zhang, Y., and Feng, Y.: Revealing Drivers of Haze Pollution by Explainable Machine Learning, Environmental Science & Technology Letters, 9, 112–119, https://doi.org/10.1021/acs.estlett.1c00865, 2022.
- Hu, Y., Zeng, C., Li, T., and Shen, H.: Performance comparison of Fengyun-4A and Himawari-8 in PM_{2.5} estimation in China, Atmospheric Environment, 271, 118898, https://doi.org/10.1016/j.atmosenv.2021.118898, 2022.
- Hua, J., Zhang, Y., de Foy, B., Mei, X., Shang, J., and Feng, C.: Competing PM_{2.5} and NO₂ holiday effects in the Beijing area vary locally due to differences in residential coal burning and traffic patterns, Science of The Total Environment, 750, 141575, https://doi.org/10.1016/j.scitotenv.2020.141575, 2021.
- Huang, C., Hu, J., Xue, T., Xu, H., and Wang, M.: High-Resolution Spatiotemporal Modeling for Ambient PM_{2.5} Exposure Assessment in China from 2013 to 2019, Environmental Science & Technology, 55, 2152–2162, https://doi.org/10.1021/acs.est.0c05815, 2021.
- Huang, R.-J., Zhang, Y., Bozzetti, C., Ho, K.-F., Cao, J.-J., Han, Y., Daellenbach, K. R., Slowik, J. G., Platt, S. M., Canonaco, F., Zotter, P., Wolf, R., Pieber, S. M., Bruns, E. A., Crippa, M., Ciarelli, G., Piazzalunga, A., Schwikowski, M., Abbaszade, G., Schnelle-Kreis, J., Zimmermann, R., An, Z., Szidat, S., Baltensperger, U., Haddad, I. E., and Prévôt, A. S. H.: High secondary aerosol contribution to particulate pollution during haze events in China, Nature, 514, 218–222, https://doi.org/10.1038/nature13774, 2014a.
- Huang, Y., Shen, H., Chen, H., Wang, R., Zhang, Y., Su, S., Chen, Y., Lin, N., Zhuo, S., Zhong, Q., Wang, X., Liu, J., Li, B., Liu, W., and Tao, S.: Quantification of Global Primary Emissions of PM_{2.5}, PM₁₀, and TSP from Combustion and Industrial Process Sources, Environmental Science & Technology, 48, 13834–13843, https://doi.org/10.1021/es503696k, 2014b.
- JMA: Himawari-8 TOAR, JMA [data set], https://www.eorc.jaxa.jp/ptree/index.html, last access: 20 September 2025.
- Li, J., Wang, Z., Zhuang, G., Luo, G., Sun, Y., and Wang, Q.: Mixing of Asian mineral dust with anthropogenic pollutants over East Asia: a model case study of a superduststorm in March 2010, Atmos. Chem. Phys., 12, 7591–7607, https://doi.org/10.5194/acp-12-7591-2012, 2012.
- Li, W., Wang, C., Wang, H., Chen, J., Yuan, C., Li, T., Wang, W., Shen, H., Huang, Y., Wang, R., Wang, B., Zhang, Y., Chen, H., Chen, Y., Tang, J., Wang, X., Liu, J., Coveney, R. M., and Tao, S.: Distribution of atmospheric particulate matter (PM) in rural field, rural village and urban areas

- of northern China, Environmental Pollution, 185, 134–140, https://doi.org/10.1016/j.envpol.2013.10.042, 2014.
- Li, X., Ye, C., Lu, K., Xue, C., Li, X., and Zhang, Y.: Accurately Predicting Spatiotemporal Variations of Near-Surface Nitrous Acid (HONO) Based on a Deep Learning Approach, Environmental Science & Technology, 58, 13035–13046, https://doi.org/10.1021/acs.est.4c02221, 2024a.
- Li, Y., Qiao, L., Liu, M., Yang, Y., Yu, F., Yuan, X., Wang, Q., Ma, Q., and Zuo, J.: Access to affordable and clean domestic heating: A critical review on rural clean heating transformation in China's Jing-Jin-Ji and its surrounding areas, Energy and Buildings, 323, 114829, https://doi.org/10.1016/j.enbuild.2024.114829, 2024b.
- Liu, J., Weng, F., and Li, Z.: Satellite-based PM_{2.5} estimation directly from reflectance at the top of the atmosphere using a machine learning algorithm, Atmospheric Environment, 208, 113–122, https://doi.org/10.1016/j.atmosenv.2019.04.002, 2019.
- Liu, P., Zhang, C., Xue, C., Mu, Y., Liu, J., Zhang, Y., Tian, D., Ye, C., Zhang, H., and Guan, J.: The contribution of residential coal combustion to atmospheric PM_{2.5} in northern China during winter, Atmos. Chem. Phys., 17, 11503–11520, https://doi.org/10.5194/acp-17-11503-2017, 2017.
- Liu, R., Ma, Z., Gasparrini, A., de la Cruz, A., Bi, J., and Chen, K.: Integrating Augmented In Situ Measurements and a Spatiotemporal Machine Learning Model To Back Extrapolate Historical Particulate Matter Pollution over the United Kingdom: 1980– 2019, Environmental Science & Technology, 57, 21605–21615, https://doi.org/10.1021/acs.est.3c05424, 2023.
- Lundberg, S. M. and Lee, S.-I.: A unified approach to interpreting model predictions, Proceedings of the 31st International Conference on Neural Information Processing Systems, Long Beach, California, USA, https://dl.acm.org/doi/pdf/10. 5555/3295222.3295230 (last access: 20 September 2025), 2017.
- Ma, S., Wang, N., Zhang, J., Ye, D., and Wang, L.: Ammonia chemistry and oxidation dynamics as dual driving factors of PM_{2.5} nitrate pollution: Insights from the spatiotemporal disparities in central China, Journal of Environmental Management, 392, 126594, https://doi.org/10.1016/j.jenvman.2025.126594, 2025.
- Ministry of Ecology and Environment of the People's Republic of China: Ambient air quality standards, https://www.mee.gov.cn/ywgz/fgbz/bz/bzwb/dqhjbh/dqhjzlbz/201203/W020120410330232398521.pdf (last access: 22 October 2024), 2012.
- Ministry of Ecology and Environment of the People's Republic of China: Report on the state of the ecology and environment in China, http://english.mee.gov.cn/Resources/Reports/soe/SOEE2017/201808/P020180801597738742758.pdf (last access: 22 October 2024), 2017.
- NASA JPL: SRTM-3, NASA Land Processes Distributed Active Archive Center [data set], https://doi.org/10.5067/MEASURES/SRTM/SRTMGL3.003, 2013.
- NASA Land Processes Distributed Active Archive Center: MCD12Q1, Land Cover Type Yearly L3 500m SIN Grid V006, NASA [data https://doi.org/10.5067/MODIS/MCD12Q1.006, 2019.
- Park, S., Shin, M., Im, J., Song, C.-K., Choi, M., Kim, J., Lee, S., Park, R., Kim, J., Lee, D.-W., and Kim, S.-K.: Estimation of ground-level particulate matter concentrations through the synergistic use of satellite observations and process-based mod-

- els over South Korea, Atmos. Chem. Phys., 19, 1097–1113, https://doi.org/10.5194/acp-19-1097-2019, 2019.
- Park, S., Lee, J., Im, J., Song, C.-K., Choi, M., Kim, J., Lee, S., Park, R., Kim, S.-M., Yoon, J., Lee, D.-W., and Quackenbush, L. J.: Estimation of spatially continuous daytime particulate matter concentrations under all sky conditions through the synergistic use of satellite-based AOD and numerical models, Science of The Total Environment, 713, 136516, https://doi.org/10.1016/j.scitotenv.2020.136516, 2020.
- Qin, K., Han, X., Li, D., Xu, J., Loyola, D., Xue, Y., Zhou, X., Li, D., Zhang, K., and Yuan, L.: Satellite-based estimation of surface NO₂ concentrations over east-central China: A comparison of POMINO and OMNO2d data, Atmospheric Environment, 224, 117322, https://doi.org/10.1016/j.atmosenv.2020.117322, 2020.
- Qiu, M., Zigler, C., and Selin, N. E.: Statistical and machine learning methods for evaluating trends in air quality under changing meteorological conditions, Atmos. Chem. Phys., 22, 10551–10566, https://doi.org/10.5194/acp-22-10551-2022, 2022.
- Qu, S., Liu, J., Li, B., Zhao, L., Li, X., Zhang, Z., Yuan, M., Niu, Z., and Lin, A.: Unveiling the driver behind China's greening trend: urban vs. rural areas, Environmental Research Letters, 18, 084027, https://doi.org/10.1088/1748-9326/ace83d, 2023.
- Rodriguez, J. D., Perez, A., and Lozano, J. A.: Sensitivity Analysis of k-Fold Cross Validation in Prediction Error Estimation, IEEE Transactions on Pattern Analysis and Machine Intelligence, 32, 569–575, https://doi.org/10.1109/TPAMI.2009.187, 2010.
- Shen, G., Ru, M., Du, W., Zhu, X., Zhong, Q., Chen, Y., Shen, H., Yun, X., Meng, W., Liu, J., Cheng, H., Hu, J., Guan, D., and Tao, S.: Impacts of air pollutants from rural Chinese households under the rapid residential energy transition, Nature Communications, 10, 3405, https://doi.org/10.1038/s41467-019-11453-w, 2019.
- Shi, S., Chen, R., Wang, P., Zhang, H., Kan, H., and Meng, X.: An Ensemble Machine Learning Model to Enhance Extrapolation Ability of Predicting Coarse Particulate Matter with High Resolutions in China, Environmental Science & Technology, 58, 19325–19337, https://doi.org/10.1021/acs.est.4c08610, 2024.
- Shi, Z., Song, C., Liu, B., Lu, G., Xu, J., Van Vu, T., Elliott, R. J. R., Li, W., Bloss, W. J., and Harrison, R. M.: Abrupt but smaller than expected changes in surface air quality attributable to COVID-19 lockdowns, Science Advances, 7, eabd6696, https://doi.org/10.1126/sciadv.abd6696, 2021.
- Sicard, P., Agathokleous, E., Anenberg, S. C., De Marco, A., Paoletti, E., and Calatayud, V.: Trends in urban air pollution over the last two decades: A global perspective, Science of The Total Environment, 858, 160064, https://doi.org/10.1016/j.scitotenv.2022.160064, 2023.
- Song, C., Liu, B., Cheng, K., Cole, M. A., Dai, Q., Elliott, R. J. R., and Shi, Z.: Attribution of Air Quality Benefits to Clean Winter Heating Policies in China: Combining Machine Learning with Causal Inference, Environmental Science & Technology, 57, 17707–17717, https://doi.org/10.1021/acs.est.2c06800, 2023.
- Song, Z.: Particulate matter data used in egusphere-2025-2194, Zenodo [data set], https://doi.org/10.5281/zenodo.17090707, 2025.
- Song, Z., Chen, B., and Huang, J.: Combining Himawari-8 AOD and deep forest model to obtain city-level distribution of PM_{2.5} in China, Environmental Pollution, 297, 118826, https://doi.org/10.1016/j.envpol.2022.118826, 2022a.

- Song, Z., Zhao, L., Ye, Q., Ren, Y., Chen, R., and Chen, B.: The Reconstruction of FY-4A and FY-4B Cloudless Top-of-Atmosphere Radiation and Full-Coverage Particulate Matter Products Reveals the Influence of Meteorological Factors in Pollution Events, https://doi.org/10.3390/rs16183363, 2024.
- Song, Z., Chen, B., Zhang, P., Guan, X., Wang, X., Ge, J., Hu, X., Zhang, X., and Wang, Y.: High temporal and spatial resolution PM_{2.5} dataset acquisition and pollution assessment based on FY-4A TOAR data and deep forest model in China, Atmospheric Research, 274, 106199, https://doi.org/10.1016/j.atmosres.2022.106199, 2022b.
- Southerland, V. A., Brauer, M., Mohegh, A., Hammer, M. S., van Donkelaar, A., Martin, R. V., Apte, J. S., and Anenberg, S. C.: Global urban temporal trends in fine particulate matter (PM_{2.5}) and attributable health burdens: estimates from global datasets, The Lancet Planetary Health, 6, e139–e146, https://doi.org/10.1016/S2542-5196(21)00350-8, 2022.
- State Council of the People's Republic of China: Action Plan on Air Pollution Prevention and Control, http://www.gov.cn/zwgk/2013-09/12/content_2486773.htm (last access: 22 October 2024), 2013.
- State Council of the People's Republic of China: Accessment Method of Air Pollution Prevention and Control Action Plan, http://www.gov.cn/zhengce/content/2014-05/27/content_8830.htm (last access: 22 October 2024), 2014.
- Vu, T. V., Shi, Z., Cheng, J., Zhang, Q., He, K., Wang, S., and Harrison, R. M.: Assessing the impact of clean air action on air quality trends in Beijing using a machine learning technique, Atmos. Chem. Phys., 19, 11303–11314, https://doi.org/10.5194/acp-19-11303-2019, 2019.
- Wang, B., Yuan, Q., Yang, Q., Zhu, L., Li, T., and Zhang, L.: Estimate hourly PM_{2.5} concentrations from Himawari-8 TOA reflectance directly using geo-intelligent long shortterm memory network, Environmental Pollution, 271, 116327, https://doi.org/10.1016/j.envpol.2020.116327, 2021.
- Wang, J., Lin, J., Liu, Y., Wu, F., Ni, R., Chen, L., Ren, F., Du, M., Li, Z., Zhang, H., and Liu, Z.: Direct and indirect consumption activities drive distinct urban-rural inequalities in air pollution-related mortality in China, Science Bulletin, 69, 544–553, https://doi.org/10.1016/j.scib.2023.12.023, 2024a.
- Wang, R., Tao, S., Ciais, P., Shen, H. Z., Huang, Y., Chen, H., Shen, G. F., Wang, B., Li, W., Zhang, Y. Y., Lu, Y., Zhu, D., Chen, Y. C., Liu, X. P., Wang, W. T., Wang, X. L., Liu, W. X., Li, B. G., and Piao, S. L.: High-resolution mapping of combustion processes and implications for CO2 emissions, Atmos. Chem. Phys., 13, 5189–5203, https://doi.org/10.5194/acp-13-5189-2013, 2013.
- Wang, W., Zhao, C., Dong, C., Yu, H., Wang, Y., and Yang, X.: Is the key-treatment-in-key-areas approach in air pollution control policy effective? Evidence from the action plan for air pollution prevention and control in China, Science of The Total Environment, 843, 156850, https://doi.org/10.1016/j.scitotenv.2022.156850, 2022a.
- Wang, X., Wang, T., Xu, J., Shen, Z., Yang, Y., Chen, A., Wang, S., Liang, E., and Piao, S.: Enhanced habitat loss of the Himalayan endemic flora driven by warming-forced upslope tree expansion, Nature Ecology & Evolution, 6, 890–899, https://doi.org/10.1038/s41559-022-01774-3, 2022b.
- Wang, Y., Hu, Y., Jiang, S., and Zhao, B.: Distinguishing urban-rural difference in Chinese population exposure to am-

- bient air pollutants, Atmospheric Environment, 334, 120704, https://doi.org/10.1016/j.atmosenv.2024.120704, 2024b.
- Wang, Y., Yu, H., Li, L., Li, J., Sun, J., Shi, J., and Li, J.: Long-term trend of dust event duration over Northwest China, Science of The Total Environment, 951, 175819, https://doi.org/10.1016/j.scitotenv.2024.175819, 2024c.
- Wei, J., Huang, W., Li, Z., Xue, W., Peng, Y., Sun, L., and Cribb, M.: Estimating 1-km-resolution PM_{2.5} concentrations across China using the space-time random forest approach, Remote Sensing of Environment, 231, 111221, https://doi.org/10.1016/j.rse.2019.111221, 2019.
- Wei, J., Li, Z., Lyapustin, A., Sun, L., Peng, Y., Xue, W., Su, T., and Cribb, M.: Reconstructing 1-km-resolution high-quality PM_{2.5} data records from 2000 to 2018 in China: spatiotemporal variations and policy implications, Remote Sensing of Environment, 252, 112136, https://doi.org/10.1016/j.rse.2020.112136, 2021a.
- Wei, J., Li, Z., Pinker, R. T., Wang, J., Sun, L., Xue, W., Li, R., and Cribb, M.: Himawari-8-derived diurnal variations in ground-level PM2.5 pollution across China using the fast spacetime Light Gradient Boosting Machine (LightGBM), Atmos. Chem. Phys., 21, 7863–7880, https://doi.org/10.5194/acp-21-7863-2021, 2021b.
- Wei, J., Li, Z., Xue, W., Sun, L., Fan, T., Liu, L., Su, T., and Cribb, M.: The ChinaHighPM10 dataset: generation, validation, and spatiotemporal variations from 2015 to 2019 across China, Environment International, 146, 106290, https://doi.org/10.1016/j.envint.2020.106290, 2021c.
- Wei, J., Li, Z., Lyapustin, A., Wang, J., Dubovik, O., Schwartz, J., Sun, L., Li, C., Liu, S., and Zhu, T.: First close insight into global daily gapless 1 km PM_{2.5} pollution, variability, and health impact, Nature Communications, 14, 8349, https://doi.org/10.1038/s41467-023-43862-3, 2023.
- Wei, J., Li, Z., Cribb, M., Huang, W., Xue, W., Sun, L., Guo, J., Peng, Y., Li, J., Lyapustin, A., Liu, L., Wu, H., and Song, Y.: Improved 1 km resolution PM_{2.5} estimates across China using enhanced space–time extremely randomized trees, Atmos. Chem. Phys., 20, 3273–3289, https://doi.org/10.5194/acp-20-3273-2020, 2020.
- West, J. J., Cohen, A., Dentener, F., Brunekreef, B., Zhu, T., Armstrong, B., Bell, M. L., Brauer, M., Carmichael, G., Costa, D. L., Dockery, D. W., Kleeman, M., Krzyzanowski, M., Künzli, N., Liousse, C., Lung, S.-C. C., Martin, R. V., Pöschl, U., Pope, C. A., III, Roberts, J. M., Russell, A. G., and Wiedinmyer, C.: "What We Breathe Impacts Our Health: Improving Understanding of the Link between Air Pollution and Health", Environmental Science & Technology, 50, 4895–4904, https://doi.org/10.1021/acs.est.5b03827, 2016.
- Xiao, Q., Zheng, Y., Geng, G., Chen, C., Huang, X., Che, H., Zhang, X., He, K., and Zhang, Q.: Separating emission and meteorological contributions to long-term PM_{2.5} trends over eastern China during 2000–2018, Atmos. Chem. Phys., 21, 9475–9496, https://doi.org/10.5194/acp-21-9475-2021, 2021.
- Xue, T., Liu, J., Zhang, Q., Geng, G., Zheng, Y., Tong, D., Liu, Z., Guan, D., Bo, Y., Zhu, T., He, K., and Hao, J.: Rapid improvement of PM_{2.5} pollution and associated health benefits in China during 2013–2017, Science China Earth Sciences, 62, 1847–1856, https://doi.org/10.1007/s11430-018-9348-2, 2019.
- Yang, J., Lin, Z., and Shi, S.: Household air pollution and attributable burden of disease in rural China: A literature review

- and a modelling study, Journal of Hazardous Materials, 470, 134159, https://doi.org/10.1016/j.jhazmat.2024.134159, 2024.
- Yang, N., Shi, H., Tang, H., and Yang, X.: Geographical and temporal encoding for improving the estimation of PM_{2.5} concentrations in China using end-to-end gradient boosting, Remote Sensing of Environment, 269, 112828, https://doi.org/10.1016/j.rse.2021.112828, 2022.
- Yang, Q., Kim, J., Cho, Y., Lee, W.-J., Lee, D.-W., Yuan, Q., Wang, F., Zhou, C., Zhang, X., Xiao, X., Guo, M., Guo, Y., Carmichael, G. R., and Gao, M.: A synchronized estimation of hourly surface concentrations of six criteria air pollutants with GEMS data, npj Climate and Atmospheric Science, 6, 94, https://doi.org/10.1038/s41612-023-00407-1, 2023.
- Yin, J., Mao, F., Zang, L., Chen, J., Lu, X., and Hong, J.: Retrieving PM_{2.5} with high spatio-temporal coverage by TOA reflectance of Himawari-8, Atmospheric Pollution Research, 12, 14-20, https://doi.org/10.1016/j.apr.2021.02.007, 2021.
- Yin, P., Brauer, M., Cohen, A. J., Wang, H., Li, J., Burnett, R. T., Stanaway, J. D., Causey, K., Larson, S., Godwin, W., Frostad, J., Marks, A., Wang, L., Zhou, M., and Murray, C. J. L.: The effect of air pollution on deaths, disease burden, and life expectancy across China and its provinces, 1990–2017: an analysis for the Global Burden of Disease Study 2017, The Lancet Planetary Health, 4, e386–e398, https://doi.org/10.1016/S2542-5196(20)30161-3, 2020.
- Yoshida, M., Kikuchi, M., Nagao, T. M., Murakami, H., Nomaki, T., and Higurashi, A.: Common Retrieval of Aerosol Properties for Imaging Satellite Sensors, J. Meteorol. Soc. Jpn. Ser. II, 96B, 193–209, https://doi.org/10.2151/jmsj.2018-039, 2018.
- Yu, Y., Dai, C., Wei, Y., Ren, H., and Zhou, J.: Air pollution prevention and control action plan substantially reduced PM_{2.5} concentration in China, Energy Economics, 113, 106206, https://doi.org/10.1016/j.eneco.2022.106206, 2022.
- Yun, X., Shen, G., Shen, H., Meng, W., Chen, Y., Xu, H., Ren, Y., Zhong, Q., Du, W., Ma, J., Cheng, H., Wang, X., Liu, J., Wang, X., Li, B., Hu, J., Wan, Y., and Tao, S.: Residential solid fuel emissions contribute significantly to air pollution and associated health impacts in China, Science Advances, 6, eaba7621, https://doi.org/10.1126/sciadv.aba7621, 2020.
- Zhai, S., Jacob, D. J., Wang, X., Shen, L., Li, K., Zhang, Y., Gui, K., Zhao, T., and Liao, H.: Fine particulate matter (PM_{2.5}) trends in China, 2013–2018: separating contributions from anthropogenic emissions and meteorology, Atmos. Chem. Phys., 19, 11031–11041, https://doi.org/10.5194/acp-19-11031-2019, 2019.
- Zhang, H., Di, B., Liu, D., Li, J., and Zhan, Y.: Spatiotemporal distributions of ambient SO₂ across China based on satellite retrievals and ground observations: Substantial decrease in human exposure during 2013–2016, Environmental Research, 179, 108795, https://doi.org/10.1016/j.envres.2019.108795, 2019a.
- Zhang, Q., He, K., and Huo, H.: Cleaning China's air, Nature, 484, 161–162, https://doi.org/10.1038/484161a, 2012.
- Zhang, Q., Shi, R., Singh, V. P., Xu, C.-Y., Yu, H., Fan, K., and Wu, Z.: Droughts across China: Drought factors, prediction and impacts, Science of The Total Environment, 803, 150018, https://doi.org/10.1016/j.scitotenv.2021.150018, 2022a.
- Zhang, Q., Zheng, Y., Tong, D., Shao, M., Wang, S., Zhang, Y., Xu,
 X., Wang, J., He, H., Liu, W., Ding, Y., Lei, Y., Li, J., Wang, Z.,
 Zhang, X., Wang, Y., Cheng, J., Liu, Y., Shi, Q., Yan, L., Geng,
 G., Hong, C., Li, M., Liu, F., Zheng, B., Cao, J., Ding, A., Gao,

- J., Fu, Q., Huo, J., Liu, B., Liu, Z., Yang, F., He, K., and Hao, J.: Drivers of improved PM_{2.5} air quality in China from 2013 to 2017, Proceedings of the National Academy of Sciences, 116, 24463–24469, https://doi.org/10.1073/pnas.1907956116, 2019b.
- Zhang, X., Brandt, M., Tong, X., Ciais, P., Yue, Y., Xiao, X., Zhang, W., Wang, K., and Fensholt, R.: A large but transient carbon sink from urbanization and rural depopulation in China, Nature Sustainability, 5, 321-328, https://doi.org/10.1038/s41893-021-00843-y, 2022b.
- Zhao, B., Zheng, H., Wang, S., Smith, K. R., Lu, X., Aunan, K., Gu, Y., Wang, Y., Ding, D., Xing, J., Fu, X., Yang, X., Liou, K.-N., and Hao, J.: Change in household fuels dominates the decrease in PM_{2.5} exposure and premature mortality in China in 2005–2015, Proceedings of the National Academy of Sciences, 115, 12401–12406, https://doi.org/10.1073/pnas.1812955115, 2018.
- Zheng, B., Tong, D., Li, M., Liu, F., Hong, C., Geng, G., Li, H., Li, X., Peng, L., Qi, J., Yan, L., Zhang, Y., Zhao, H., Zheng, Y., He, K., and Zhang, Q.: Trends in China's anthropogenic emissions since 2010 as the consequence of clean air actions, Atmos. Chem. Phys., 18, 14095–14111, https://doi.org/10.5194/acp-18-14095-2018, 2018.

- Zheng, H., Kong, S., He, Y., Song, C., Cheng, Y., Yao, L., Chen, N., and Zhu, B.: Enhanced ozone pollution in the summer of 2022 in China: The roles of meteorology and emission variations, Atmospheric Environment, 301, 119701, https://doi.org/10.1016/j.atmosenv.2023.119701, 2023.
- Zhong, Q., Ma, J., Shen, G., Shen, H., Zhu, X., Yun, X., Meng, W., Cheng, H., Liu, J., Li, B., Wang, X., Zeng, E. Y., Guan, D., and Tao, S.: Distinguishing Emission-Associated Ambient Air PM_{2.5} Concentrations and Meteorological Factor-Induced Fluctuations, Environmental Science & Technology, 52, 10416–10425, https://doi.org/10.1021/acs.est.8b02685, 2018.
- Zhong, Q., Tao, S., Ma, J., Liu, J., Shen, H., Shen, G., Guan, D., Yun, X., Meng, W., Yu, X., Cheng, H., Zhu, D., Wan, Y., and Hu, J.: PM_{2.5} reductions in Chinese cities from 2013 to 2019 remain significant despite the inflating effects of meteorological conditions, One Earth, 4, 448–458, https://doi.org/10.1016/j.oneear.2021.02.003, 2021.